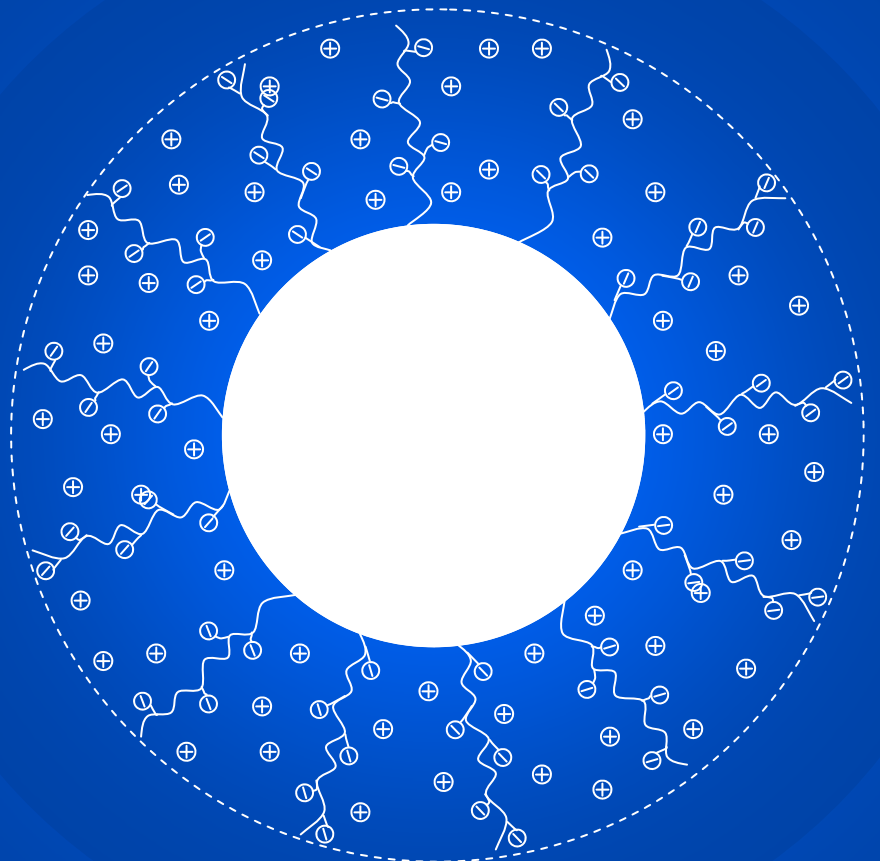


Water activity measurements of a system of poly(styrene-*co*-sodium acrylate) core-shell particles and water



Master's Thesis
Katrine Skelbæk Christiansen
September 2008 - June 2009

Faculties of Engineering, Science and Medicine

Aalborg Universitet

Department of Biotechnology, Chemistry and Environmental Engineering
Section of Chemistry

Title

Water activity measurements of a system of poly(styrene-*co*-sodium acrylate) core-shell particles and water

Project period

September 2008 - June 2009

Composed by

Katrine Skelbæk Christiansen

Supervisor

Associate professor Kristian Keiding

Issues: 3

No of pages: 83

No of appendices: 4

CD-ROM

Katrine Skelbæk Christiansen

Abstract

Core-shell particles are widely studied due to a variety of possible application. Especially for polyelectrolyte core-shell particles the interaction with water has been studied. Though polyelectrolyte core-shell particles have never been investigated by water activity measurements in the concentrated range. Hence this study focus on the use of water activity measurements to describe the interaction between core-shell particles of poly(styrene-*co*-sodium acrylate) (PS-NaPAA) and water.

The water activity has been measured for PS-NaPAA particles both as a function of water content and temperature. For comparison sodium polyacrylate, sodium acrylate, bare polystyrene particles and protonated poly(styrene-*co*-acrylic acid) have been measured as a function of water content.

The results show that the water activity for PS-NaPAA is determined mainly by the charges and counterions in the shell. Additionally the measured water activity as a function of water content indicate a water content below which the system can be described by adsorption. Above this point the system can be described as a suspension.

From the measurements of the water activity as a function of temperature an excess enthalpy necessary to evaporate the water from the samples of PS-NaPAA is determined. The behaviour of this excess enthalpy as a function of water content is confirmed by a drying experiment.

It is concluded that water activity measurements can be used to describe the interactions between polyelectrolyte core-shell particles and water.

1. Synopsis

Kerneskalpartikler har en række mulige anvendelser og er derfor studeret af mange. Interaktionerne mellem kerneskalpartikler og vand er specielt blevet undersøgt for kerneskalpartikler med en polyelektrolytskal. Dog er vandaktivitetsmålinger aldrig blevet brugt til undersøgelse af disse interaktioner for koncentrerede suspensioner. Formålet med dette projekt er således at bruge vandaktivitetsmålinger til at bestemme interaktionerne mellem poly(styren-*co*-natriumacrylate) (PS-NaPAA) kerneskalpartikler og vand.

Vandaktiviteten er blevet målt for PS-NaPAA partikler både som funktion af vandindholdet og temperaturen. Til sammenligning er natriumpolyacrylate, polystyren partikler, natriumacrylate og protoneret poly(styren-*co*-acrylsyre) målt som funktion af vandindholdet.

Resultaterne viser, at det hovedsageligt er skallen med dens ladninger og modioner, der er bestemmende for vandaktiviteten af PS-NaPAA. Desuden indikerer vandaktivitetsmålingerne som funktion af vandindhold et vandindhold, under hvilket systemet kan beskrives med adsorption. Over dette punkt kan systemet betragtes som en suspension.

Fra vandaktivitetsmålingerne som funktion af temperatur er den ekstra entalpi, der er nødvendigt for at fordampe vandet fra PS-NaPAA, bestemt. Variationen af denne entalpi som funktion af vandindholdet er delvist bekræftet af et tørringsforsøg.

Det kan konkluderes, at vandaktivitetsmålinger kan bruges til at beskrive interaktionerne mellem polyelektrolyt kerneskalpartikler og vand.

Projekttitel: Vandaktivitetsmålinger for et system af poly(styren-*co*-natriumacrylate) kerneskalpartikler og vand.

2. Preface

This master thesis is composed at Aalborg University, Department of Biotechnology, Chemistry and Environmental Engineering, Section of Chemistry in the period September 2008 - June 2009. The focus of this report is "Water activity measurements of a system of poly(styrene-*co*-sodium acrylate) core-shell particles and water".

The equations, tables and figures are numbered continuously in each chapter. The references is given as [author, publication year].

All raw data and calculations is found on the attached CD-ROM. Additionally an electronic version of this report can be found on the CD-ROM.

The author wishes to thank Jonas Laursen for synthesis of core-shell particles.

Contents

1	Synopsis	5
2	Preface	7
3	Introduction	11
4	Theory	13
4.1	Water activity and osmotic pressure	13
4.2	Polyelectrolyte solutions	14
4.3	Adsorption	18
4.4	A theory for interpretation of water activity	22
4.5	Core-shell particles	23
5	Experimental approach	25
6	Methods	27
6.1	Determination of dry matter content	27
6.2	Size determination by dynamic light scattering	27
6.3	Determination of water activity	28
6.4	Osmotic pressure by membrane osmometry	29
6.5	Drying by simultaneous thermal analysis	30
7	Results	31
7.1	Initial characterisation of the particles	31
7.2	Water activity as a function of water content	32
7.3	Water activity as a function of temperature	51
7.4	Drying of poly(styrene- <i>co</i> -sodium acrylate)	54
8	Discussion	57
8.1	Validation of methods	57
8.2	Deviations in water activity between like samples	58
8.3	Interpretation of a_w as function of water content	59
8.4	The different parts contribution to a_w	61

8.5	Interpretation of the osmotic coefficient	62
8.6	The excess enthalpy	63
9	Conclusion	65
	Bibliography	66
	Appendix	72
A	Calculation of particle characteristics	73
A.1	The number of particles	73
A.2	The size of the poly(acrylic acid) chains	74
A.3	Charges per particle	75
A.4	The volume of water in the shell	75
B	Sample stability during freezedrying	77
B.1	Flocculation study	77
B.2	pH for resuspended poly(styrene- <i>co</i> -sodium acrylate)	78
B.3	Conclusion	79
C	Effect of sample storage	80
C.1	Method	80
C.2	Results	80
C.3	Conclusion	82
D	Day of measurement	83

3. Introduction

Many systems in our every day life contains morphologies resembling core-shell particles. These include soil, which is minerals with a soft charged polymeric surface layer among others [Ellerbrock et al., 2005], and sewage sludge [Christensen, 2008]. Core-shell particles are also produced artificially as core-shell particles have properties different from the properties of the core and shell material separately [Wu et al., 2008, Small et al., 2005]. Artificial core-shell particles can be used for e.g. coatings as core-shell particles with one film forming polymer is enough to make film formation possible [Kan et al., 2001] and hence the other polymer can provide the film some extra strength, resistance etc. Core-shell particles can also be used for rubber-strengthening, adhesives and impact-resistance plastic [Wu et al., 2008].

Due to the many systems containing core-shell like structures and the many applications of core-shell particles research has been done to investigate the behaviour and properties of core-shell particles to get a thorough understanding of core-shell particles in different systems. Thus the structure and morphology of core-shell particles are widely studied [Semenov et al., 1999, Wu et al., 2008, Kan et al., 2001] along with the water uptake in a dry films of core-shell particles [Wu et al., 2008, Kan et al., 2001]. Additionally, core-shell particles with polyelectrolyte shell are studied in suspension regarding stability and flocculation [Fritz et al., 2002, Borget et al., 2005] and determination of osmotic coefficients [Das et al., 2002]. The last two properties concern polyelectrolyte core-shell particles interaction with water which is important since polyelectrolyte core-shell particles are always considered in aqueous suspension.

One way to measure the behaviour of water associated with core-shell particles is to measure the water activity (a_w). The term water activity is used to describe the effective amount of water in a given mixture or solution [Chaplin, 2008] and is defined as $a_w = P_{aq}/P_{aq}^*$ [Blandamer et al., 2005]. The water activity reflects both the colligative properties of a system along with the specific interactions between water and solutes as well as surfaces of e.g. colloids dispersed in the water [Chaplin, 2008]. Therefore water activity measurements can provide an understanding of the osmotic pressure associated with suspensions of polyelectrolyte core-shell particles as well as drying and adsorption behaviour of core-shell particles. For example water activity measurements may give information on the extent of the hydration of polyelectrolyte core-shell particles.

No reports on water activity or osmotic pressure measurements for polyelectrolyte core-shell particles in the concentrated range have been found in the literature and only few reports concerning the osmotic pressure for dilute suspensions [Das et al., 2002]. Hence

the focus of this project is to measure the water activity of polyelectrolyte core-shell particles in order to answer the following question:

Is it possible to obtain information on the interactions between polyelectrolyte core-shell particles and water by water activity measurements?

The measurements will be conducted on a model system of poly(styrene-*co*-acrylic acid) core-shell (PS-PAA) particles. The particles will be investigated mainly in their deprotonated form i.e. with a shell of sodium polyacrylate. PS-PAA particles in the protonated form will be measured as well to obtain information of the charges and the counterions impact on the water activity. Additionally model substances for the different parts of the particles will be measured individually in order to determine the different parts impact on the water activity. For all samples the water activity will be measured by a chilled-mirror dewpoint method at different concentrations. Additionally the particles of poly(styrene-*co*-sodium polyacrylate) (PS-NaPAA) will be investigated at different temperatures. For dilute suspensions the osmotic pressure will be measured using membrane osmometry. For comparison a sample of PS-NaPAA particles will be dried using thermogravimetry.

4. Theory

In order to be able to interpret the measured water activity it is necessary to review the relevant theory. Hence this chapter starts with a short summary of the definition of water activity and osmotic pressure. As the water activity for PS-NaPAA particles will be measured in a large concentration range the system may be partly described by the theory for polyelectrolyte solutions and partly by adsorption theory, hence this chapter proceed with descriptions of both theories. Additionally an interpretation of the water activity for a polyelectrolyte-water system is given. Finally the relevant research results for core-shell particles are reviewed.

4.1 Water activity and osmotic pressure

As mentioned the water activity is defined as [Blandamer et al., 2005]

$$\begin{aligned} a_w &= \frac{P_{aq}(T)}{P_{aq}^*(T)} \\ &= \frac{RH}{100} \end{aligned} \quad (4.1)$$

where P_{aq} is the partial water vapour pressure, P_{aq}^* is the saturated water vapour pressure at the same temperature and RH is the relative humidity in percentage.

The water activity can also be expressed as [Blandamer et al., 2005]

$$a_w = \gamma_w x_w \quad (4.2)$$

where γ_w is the activity coefficient of water and x_w is the mole fraction of water. Hence x_w describe the colligative part of a_w and γ_w describe the specific interactions between water and the solutes.

The chemical potential of water is related to the water activity of a given mixture by [Blandamer et al., 2005]

$$\mu = \mu^* + RT \ln a_w \quad (4.3)$$

where μ is the chemical potential of water in the solution/suspension, μ^* is the chemical potential of pure water, R is the gas constant, T is the temperature and a_w is the water activity.

The relation between the change in the chemical potential of water and the chemical potential of the solutes is given by the Gibbs-Duhem equation [Atkins and de Paula, 2002]

$$\sum n_i d\ln\mu_i = 0 \quad (4.4)$$

where n_i is the number of moles of specie i and μ_i is the chemical potential of specie i . Hence a change in the chemical potential for water is compensated by a change in the chemical potential for the solutes.

The water activity is related to the osmotic pressure as [Chang, 2000]

$$\Pi = \frac{RT}{\hat{V}_m} \ln a_w \quad (4.5)$$

where Π is the osmotic pressure, R is the gas constant, T is the temperature, \hat{V}_m is the partial molar volume of water and a_w is the water activity.

4.2 Polyelectrolyte solutions

A polyelectrolyte in water consist of a polyion and its counterions [Vlachy, 2008]. The counterions are associated with the polyion either by attractive coulombic forces, called physical association, or by specific site-binding, called chemical association [Daoust and Hade, 1976]. In the former binding type the counterions are not bonded to the polyion whereas in the latter binding type the counterions are chemically bounded to the charged groups on the polyions and hence the overall charge is reduced [Daoust and Hade, 1976]. Counterions chemically associated with the polyion are also referred to as condensed [Manning, 1969]. The main difference between physical and chemical association is that the charge on the polyion and the counterion are both hydrated when physical associated whereas the specific site-binding generally results in a dehydration of the charges [Daoust and Hade, 1976]. The identity of the counterions greatly influences the properties of the polyelectrolyte as do the identity of the charged and uncharged groups on the polyion [Vlachy, 2008]. The counterions influence on the properties can be attributed to the degree of hydration of the counterions [Vlachy, 2008, Daoust and Hade, 1976] and to the energy needed to release the from the polyion [Daoust and Hade, 1976].

4.2.1 Charge density parameter

One way to model the amount of counterions chemically associated with the polyelectrolyte is the charge density parameter [Manning, 1969]. The charge density parameter is the Bjerrum length divided by the distance between the charges on the polyion

[Manning, 1969] and hence it is defined as [Vlachy, 2008]

$$\xi = \frac{e_0^2}{4\pi\epsilon_0\epsilon_r k_B T b} \quad (4.6)$$

where e_0 denotes the elemental charge, ϵ_0 is the dielectric constant of vacuum, ϵ_r is the relative dielectric constant of the solvent, k_B is Boltzmann constant, T is the temperature and b is the distance between charges projected to the stretched backbone of the polyion. The Bjerrum length is defined as the distance between charges where the electrostatic interaction energy equals the thermal energy $k_B T$ [Das et al., 2002]. If the charge density parameter is below one the distance between two charges on the polyion is longer than the Bjerrum length and the system is stable. If the charge density parameter is above one the polyion charges have an unfavourable interaction which can be compensated by counterion condensation until the charge density parameter is below one [Manning, 1969]. This theory for ion condensation is derived for infinite dilute solutions which is not practical obtainable [Manning, 1984] and therefore the charge density parameter can not be used quantitatively [Blaul et al., 2000]. Though the theory can still be used in a qualitative manner [Blaul et al., 2000].

4.2.2 Osmotic coefficient

An often used parameter to describe polyelectrolytes interaction with water is the osmotic coefficient [Vlachy, 2008]. The osmotic coefficient relates the the real osmotic pressure to that of the ideal solution, hence it is given by [Vlachy, 2008]

$$\varphi = \frac{\Pi_{real}}{\Pi_{ideal}} = \frac{\ln a_w}{\ln x_w} \quad (4.7)$$

where φ is the osmotic coefficient, Π is the osmotic pressure, a_w is the water activity and x_w is the mole fraction of water. Since the osmotic coefficient is calculated as the natural logarithm to the water activity and the mole fraction of water, a small deviation in the water activity results in a larger deviation in the osmotic coefficient.

The osmotic coefficient has been interpreted in several ways. When it is assumed that bound counterions do not contribute to the osmotic pressure, the osmotic coefficient correspond to the fraction of free counterions [Rice and Nagasawa, 1961]. Manning [1969] does not agree with this interpretation since his calculations show that $(1-\varphi)$ is not simply the fraction of counterions condensed on the polyelectrolyte but rather a combination of condensed counterions and Debye Hückel interactions on the free counterions. Nevertheless the osmotic coefficient is still today interpreted as the fraction of free counterions at infinite dilution [Filho and Maurer, 2008]. As seen in equation 4.7 the osmotic coefficient

is correlated to the water activity and hence Vlachy [2008] interprets an increase in osmotic coefficient as a stronger hydration of solutes. The osmotic coefficient is only slightly dependent on the nature of the counterions [Vlachy, 2008].

For polyelectrolyte core-shell particles the osmotic coefficient of dilute solutions can be regarded as the fraction of counterions which are not trapped in the shell of the core-shell particles [Das et al., 2002].

4.2.3 A model for osmotic coefficient of polyelectrolytes

It is desirable to model the water activity measurements for the particles in suspension by a model based on the theory for polyelectrolyte solutions. From such a model it will be possible to distinguish the concentration range for which the particle-water system is described by the theory for polyelectrolyte solutions. Additionally such a model may provide some information of the activity coefficients for the counterions and the particles (polyions) and hence by use of the Gibbs-Duhem equation give an idea of whether it is the polyion or the counterions that causes the changes in water activity.

One attempt to model the non-ideality of polyelectrolyte solutions has been made by Filho and Maurer [2008] who has developed a semiempirical model for the osmotic coefficients of polyelectrolyte solutions. The model by Filho and Maurer [2008] is based on the model derived by Pitzer [1973] for simple electrolytes along with polyelectrolyte theory derived by Manning [Filho and Maurer, 2008]. Filho and Maurer [2008] had shown that this model fits adequately to measured osmotic coefficients for e.g. sodium polyacrylate, hence this model will be used to fit to the measurements in this project. In the following the model by Filho and Maurer [2008] will be described followed by a brief discussion of the limitations of the model.

The theoretical osmotic coefficient which must be fitted to the experimentally determined osmotic coefficient are calculated as [Filho and Maurer, 2008]

$$\varphi = \frac{-M_w m_p (1 + \sigma) + 2A_\varphi M_w \frac{I^{1.5}}{1+b\sqrt{I}} - 2M_w (\lambda_{c,p}^0 + \lambda_{c,p}^1 \exp(-\alpha\sqrt{I})) m_c m_p}{-M_w m_p (1 + r_p)} \quad (4.8)$$

where M_w is the molar mass of water, m_p is the molal concentration of polymer, σ is the number of free charges per polyelectrolyte, A_φ is the Debye-Hückel parameter which is $0.3914 \text{ kg}^{0.5} \text{ mol}^{-0.5}$ at $25 \text{ }^\circ\text{C}$ [Filho and Maurer, 2008], I is the ionic strength, b is a constant equal to $1.2 \text{ kg}^{0.5} \text{ mol}^{-0.5}$ at $25 \text{ }^\circ\text{C}$ [Pitzer, 1973], $\lambda_{c,p}^0$ and $\lambda_{c,p}^1$ are interaction parameters, α is a constant equal to $2.0 \text{ kg}^{0.5} \text{ mol}^{-0.5}$ [Pitzer, 1973], m_c is the molal counterion concentration and r_p is the number of monomers per polyion.

As the osmotic coefficient is calculated according to equation 4.7 the numerator in equation 4.8 corresponds to $\ln a_w$ whereas the denominator corresponds to $\ln x_w$ where all

counterions and polyions is taking into account [Filho and Maurer, 2008].

The expression for $\ln a_w$ can be split into three contributions. The first term in the numerator corresponds to $\ln x_w$ taking only the free counterions and the polyions into account. The second and third term are expressions for $\ln \gamma_w$ derived from the excess Gibbs energy [Filho and Maurer, 2008]. The excess Gibbs energy regards the interaction between the solutes [Filho and Maurer, 2008]. As depicted in figure 4.1 three different interaction pairs are present: counterion-counterion, polyion-polyion and polyion-counterion. The model by Filho and Maurer [2008] regards only the the interaction between unlike charges ions i.e. the polyion-counterion interaction which is depicted by

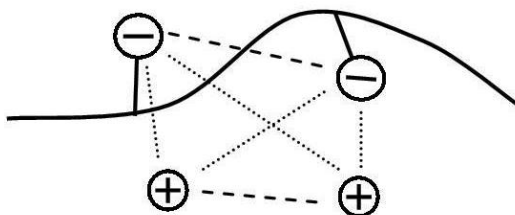


Figure 4.1: A part of a polyion and the corresponding counterions. The interactions between the charged of the same sign (---) and unlike sign (···) is depicted.

the small dotted lines in figure 4.1. A part of the interactions between the ions can be attributed to coulomb forces [Filho and Maurer, 2008]. This part is denoted the long range interactions and is described by the second term in the numerator in equation 4.8 [Filho and Maurer, 2008]. The remaining part of the interactions is denoted the short range interaction [Filho and Maurer, 2008] and is given by the third term in the numerator in equation 4.8.

m_c is calculated as $m_c = \sigma m_p$. σ is calculated as r_p times the fraction of free counterions ϵ_p . ϵ_p is assumed to be independent of concentration [Filho and Maurer, 2008] and is obtained as the osmotic coefficient at infinite dilution i.e. the limiting osmotic coefficient [Filho and Maurer, 2008]. The ionic strength is calculated as [Filho and Maurer, 2008]

$$I = 0.5 \sum m_i \sigma_i z_i^2 \quad (4.9)$$

where m_i is the molal concentration of solute i , σ_i is the number of charged groups per molecule of i and z_i is the valence of each charged group.

When $\lambda_{c,p}^0$ and $\lambda_{c,p}^1$ is determined by fitting equation 4.8 to the experimental data, the activity coefficients for the counterions and the polyions can be calculated according to equation 4.10-4.13. As for the water the activity coefficients it divided into a long range and a short range activity coefficient. The long range activity coefficient is calculated as

[Filho and Maurer, 2008]

$$\ln\gamma_i^{LR} = -A_\varphi\sigma_i z_i^2 \left(\frac{2}{b} \ln(1 + b\sqrt{I}) + \frac{\sqrt{I}}{1 + b\sqrt{I}} \right) \quad (4.10)$$

where γ_i^{LR} is the activity coefficient for specie i regarding the the long range interaction. The similar expression for the short range activity coefficient is [Filho and Maurer, 2008]

$$\ln\gamma_i^{SR} = 2(\lambda_{c,p}(I)m_i + \lambda_{c,p}(I)m_j) \quad (4.11)$$

where $\lambda_{c,p}(I)$ is calculated as [Filho and Maurer, 2008]

$$\lambda_{c,p}(I) = \lambda_{c,p}^0 + \lambda_{c,p}^1 \frac{2}{\alpha^2 I} (1 - (1 + \alpha\sqrt{I})\exp(-\alpha\sqrt{I})) \quad (4.12)$$

From equation 4.10-4.12 the activity coefficient of the counterions and the polyions can be calculated as

$$\gamma_i = \gamma_i^{LR}\gamma_i^{SR} \quad (4.13)$$

Since the values of the calculated activity coefficients for the counterions and the polyions are determined by the model, the proportion between the activity coefficients for counterions and polyions depends only on the model and not on the real system. Thus the model cannot be used to describe the actual correlation between counterions, polyelectrolyte and water in the system.

As noted the Filho and Maurer model is semiempirical. Hence the model must be fitted to measurements in a concentration range for which the particles is clearly in suspension. Thus the concentration range in which the particle suspension behaves like a polyelectrolyte suspension can be interpreted as the concentration range for which the model approaches the measurements.

4.3 Adsorption

Most theory for adsorption is concerned with the adsorption of a gas to a solid. Even though the system under investigation consist of liquid water and a solid the theory for gas adsorption must still be applicable since the liquid water is in equilibrium with water vapour.

4.3.1 Types of adsorption

Adsorption of a gas to a solid can be examined by studying the adsorption isotherms for the system. Normally the isotherms are one of the types shown in figure 4.2

[Hiemenz and Rajagopalan, 1997, Lyklema, 1995]. The amount of adsorbed gas is given as a volume in figure 4.2 but other quantities are equally usable [Lyklema, 1995].

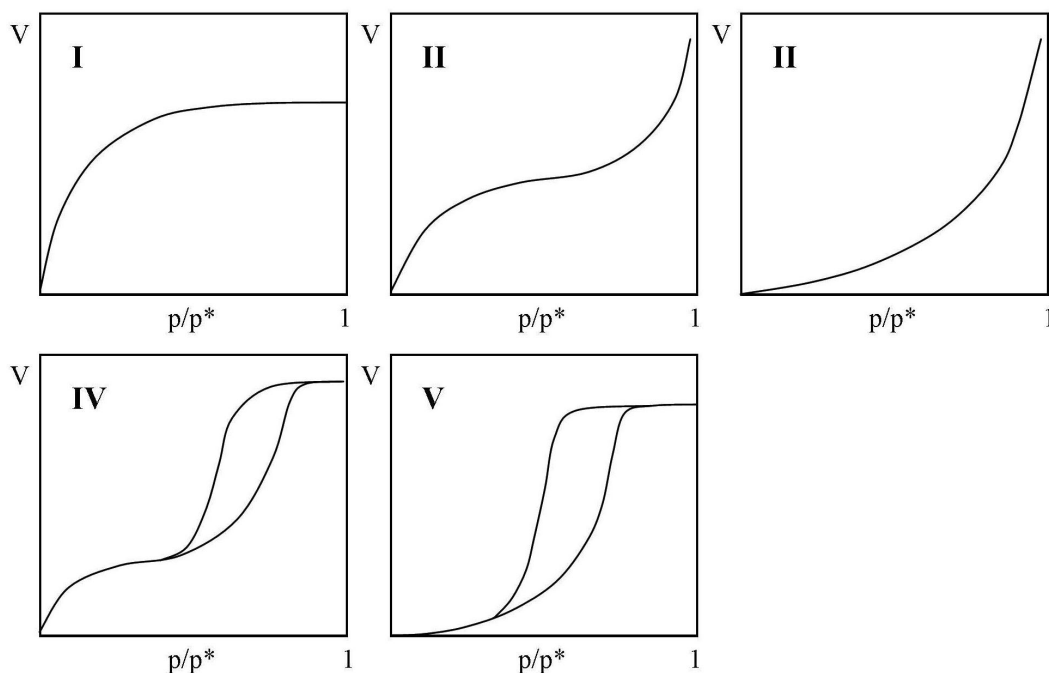


Figure 4.2: The five general isotherms for adsorption. The isotherm is plotted as the volume of adsorbed gas as a function of the relative pressure.

Type I is observed for monolayer adsorption i.e. when only one layer of adsorbate is adsorbed [Hiemenz and Rajagopalan, 1997]. Additionally this type of adsorption is observed for microporous solid [Lyklema, 1995]. Type II is observed for multilayer adsorption i.e. there is no upper limit for the adsorbed amount of gas [Hiemenz and Rajagopalan, 1997]. Type III corresponds to multilayer adsorption where the enthalpy of adsorption is less negative than the enthalpy of liquefaction [Hiemenz and Rajagopalan, 1997]. Both type II and III are observed for adsorption of gas onto non-porous or macroporous adsorbents [Lyklema, 1995]. Type IV and V are adsorption isotherms similar to II and III respectively, but for porous adsorbents [Hiemenz and Rajagopalan, 1997]. The upper limit for adsorption observed in type IV and V is due to condensation of gas in the pores [Hiemenz and Rajagopalan, 1997]. The hysteresis loops results from the different behaviour of adsorption and desorption due to the pores [Lyklema, 1995].

4.3.2 BET isotherm

Many efforts have been made to model the different isotherm in order to achieve insight into the physical characteristics of the systems investigated [Lyklema, 1995]. In the fol-

lowing the BET isotherm is described as it is one of the most widely used isotherms for multilayer adsorption, which is the most common type of adsorption of a gas to a solid [Lyklema, 1995]. The BET isotherm can describe both type II and III adsorption [Lyklema, 1995].

The BET isotherm is derived by evaluating the rate of adsorption and desorption for multiple layers [Hiemenz and Rajagopalan, 1997]. The resulting equation is [Atkins and de Paula, 2002]

$$V/V_{mono} = \frac{c \cdot x}{(1 - x)(1 + (c - 1)x)} \quad (4.14)$$

where V is the adsorbed volume, V_{mono} is the volume in the monolayer, x is the relative pressure i.e. for water $x = a_w$ and c is a constant defined as [Atkins and de Paula, 2002]

$$c = e^{\frac{\Delta H_{des} - \Delta H_{vap}}{RT}} \quad (4.15)$$

where ΔH_{des} and ΔH_{vap} is the enthalpy of desorption and vaporization respectively, R is the gas constant and T is temperature. In equation 4.14 the amount of adsorbed gas is given as a volume but other quantities are equally valid e.g. if the gas is water vapour the water content Y can be used.

The BET isotherm can be rewritten to obtain the relative pressure as a function of the amount of adsorbed gas. This conversion is given in equation 4.16 for adsorption of water to a solid i.e. x is substituted by a_w and V is substituted by Y .

$$a_w = \frac{Yc - 2Y - Y_{mono}c + (Y^2c^2 - 2YY_{mono}c^2 + 4YY_{mono}c + Y_{mono}^2c^2)^{0.5}}{2(Yc - Y)} \quad (4.16)$$

Equation 4.16 is denoted the inverted BET isotherm and can be used to describe the water activity as a function of the water content. The isotherm corresponding to equation 4.16 is given in figure 4.3 along with an isotherm corresponding to equation 4.14.

According to equation 4.14 or 4.16 and 4.15 the BET isotherm can give values for both the enthalpy of desorption and the amount of e.g. water in the monolayer. Though the determination of $\Delta H_{des} - \Delta H_{vap}$ from c according to equation 4.15 provides only a rough estimate, as c additionally include any entropic contribution and deviations of the adsorption pattern between the model and the system [Lyklema, 1995]. The deviation in adsorption pattern can be due to heterogeneity of the solid surface [Lyklema, 1995].

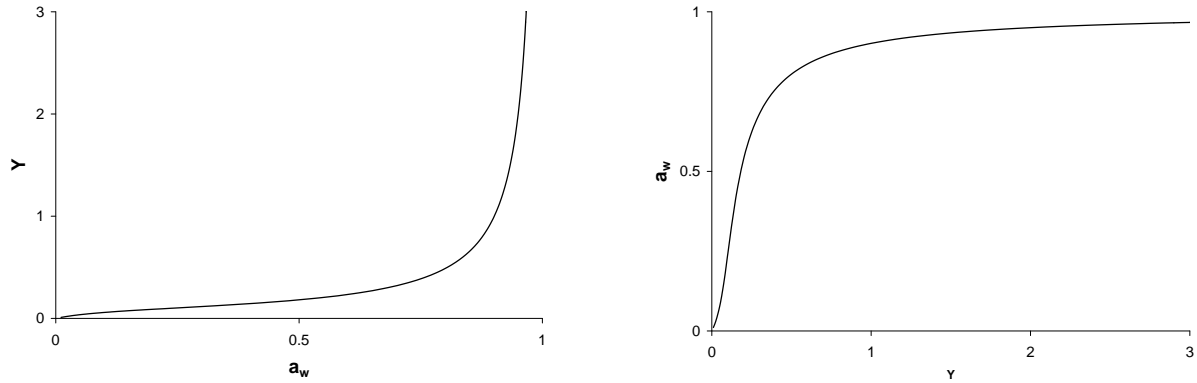


Figure 4.3: *Left:* The BET isotherm for water content as a function of water activity. *Right:* The inverted BET isotherm for water activity as a function of water content. $Y_{mono} = 0.1$ and $c = 10$.

4.3.3 Isosteric enthalpy of adsorption

The isosteric enthalpy of adsorption is the enthalpy of adsorption of a gas to a solid with a constant coverage of the solid [Hiemenz and Rajagopalan, 1997]. Hence the equilibrium under investigation is



where g denoted gas and ads denote adsorbed. The isosteric enthalpy of adsorption for the system described by equation 4.17 can be determined by [Atkins and de Paula, 2002]

$$\frac{d \ln p}{d(1/T)} = \frac{\Delta H_{ads}}{R} \quad (4.18)$$

where p is the pressure of the gas, T is the temperature, ΔH_{ads} is the isosteric enthalpy of adsorption and R is the gas constant. Hence the isosteric enthalpy of adsorption can be calculated from the slope of a straight line of $\ln p$ vs. $\frac{1}{T}$.

By substituting p in equation 4.18 by the expression for p given by the definition of water activity in equation 4.1 the following rewriting is made

$$\frac{d(\ln a_w + \ln p^*)}{d(1/T)} = \frac{\Delta H_{ads}}{R} \quad (4.19)$$

$$\begin{aligned} & \Downarrow \\ \frac{d \ln a_w}{d(1/T)} + \frac{d \ln p^*}{d(1/T)} &= \frac{\Delta H_{ads}}{R} \end{aligned} \quad (4.20)$$

As the term containing p^* is known to give the condensation enthalpy divided by the gas constant, the enthalpy of adsorption can be separated into a part concerning the condensation enthalpy and a part concerning the excess enthalpy due to adsorption of gas

to solid. Hence equation 4.19 is rearranged to

$$\frac{d \ln a_w}{d(1/T)} + \frac{d \ln p^*}{d(1/T)} = \frac{\Delta H_{excess}}{R} + \frac{\Delta H_{con}}{R} \quad (4.21)$$

where ΔH_{excess} and ΔH_{con} denote excess and condensation enthalpy respectively. Hence ΔH_{excess} can be obtained by fitting a straight line to a plot of $\ln a_w$ vs. $\frac{1}{T}$. ΔH_{excess} can also be obtained from the slope of the straight line of $\ln \gamma_w$ vs. $\frac{1}{T}$ since $a_w = x_w \gamma_w$ and x_w is independent of the temperature.

The negative excess enthalpy is also denoted the net isosteric heat of sorption [Mulet et al., 1999].

Note that in theory ΔH_{excess} has the same numerical value but the opposite sign as $\Delta H_{des} - \Delta H_{vap}$ which can be obtained from a BET fit.

4.4 A theory for interpretation of water activity

In the following a theory for the interpretation of the relationship between relative humidity and concentration for polyelectrolyte solutions is given. As the relative humidity is simply the water activity in percentage this theory may be useful for the interpretation of the measurements in this study.

Thijs and coworkers [2007] had measured the weight change for dried samples of polyelectrolytes exposed to air with different relative humidities. The results for sodium polyacrylate (particle size $<1000 \mu\text{m}$) and poly(acrylic acid) ($M_n=1800 \text{ g/mol}$) is shown in figure 4.4. The samples of sodium polyacrylate is observed to have almost constant

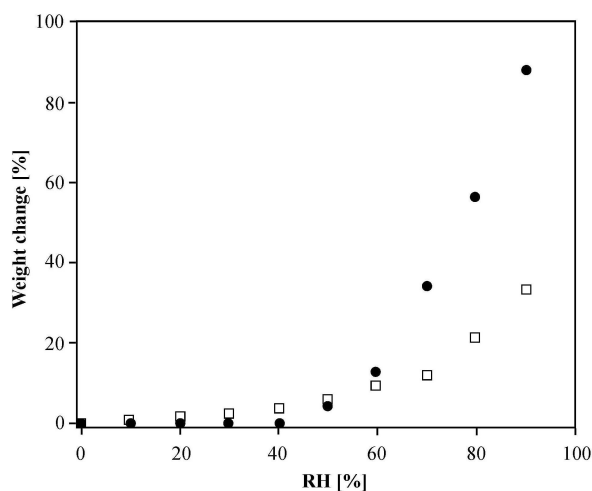


Figure 4.4: The weight change for samples of poly(acrylic acid) (●) and sodium polyacrylate (□) as a function of relative humidity according to Thijs and coworkers [2007].

weight at $RH < 40\%$ above which a gradually larger increase in weight change per RH is observed with increasing RH. For PAA the weight change per increase in RH is gradually increased as RH increases but less pronounced than for sodium polyacrylate.

According to Thijs and coworkers [2007] the almost constant weight of at low RH may be caused by a conformation of the polymer for which water interaction is unfavorable. To compensate for the energy needed to change the polymer conformation to a conformation for which hydration is more favorable the first hydration shell must be formed [Thijs et al., 2007]. When the conformation is changed water is much easier adsorbed to the polymers and hence the water uptake increases at higher RH.

4.5 Core-shell particles

The core-shell particles used in this study has no added crosslinker and hence the poly(acrylic acid) (PAA) in the shell is assumed to be linear polymers with one end attached to the polystyrene core. This type of core-shell particles are sometimes referred to as spherical polyelectrolyte brushes [Das et al., 2002].

The size of the core-shell particles depends on the charge of the shell and the elasticity of the polyelectrolyte chains, as the counterions in the shell increase the osmotic pressure and thereby draws water into the shell [Guo and Ballauff, 2001]. Since PAA is a weak polyelectrolyte the charge of the shell and hence the size of the particles depends on pH. For polystyrene colloids with poly(acrylic acid) brush the size is found to increase in the range pH 3-9 above which the shell is completely swollen i.e. the poly(acrylic acid) chains is fully stretched and hence constant [Guo and Ballauff, 2000]. Below pH 3 the shell is collapsed [Guo and Ballauff, 2000]. A schematic representation of the charged core-shell particle is shown in figure 4.5.

The counterions in a suspension of core-shell polyelectrolyte colloids can be classified into three groups: Ions condensed on the polyelectrolyte i.e. chemically associated ions, ions which can move freely within the shell but not leave the shell, and ions which are not confined to the shell [Dingenouts et al., 2004]. The three groups of counterions is depicted at A, B, and C in figure 4.5 respectively.

Small-angle neutron scattering measurements on isotop labeled counterions in copolymeric micelles with a polyelectrolyte coronal layer had shown that all counterions with a 10 % error margin were trapped within the coronal layer [Groenewegen et al., 2000]. Dingenouts and coworkers [2004] have used anomalous small-angle x-ray scattering to show that the counterions in polyelectrolyte brushes follow the distribution of polyelectrolyte i.e. counterions are confined within the coronal layer. Osmotic coefficient determinations for core-shell particles in dilute suspensions confirm the trapping of counterions in the

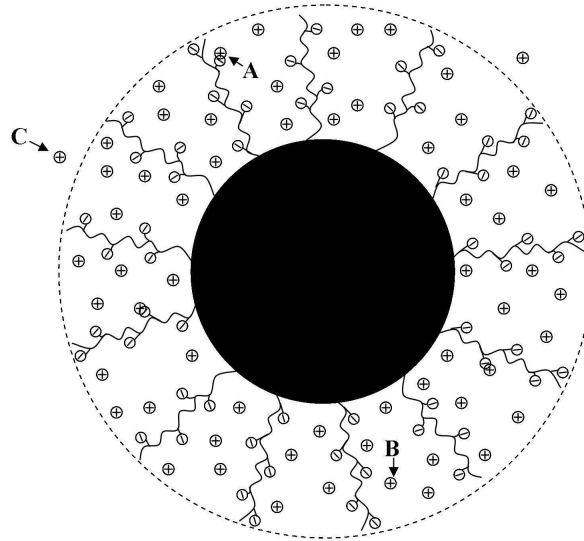


Figure 4.5: A schematic representation of a charged core-shell particle. The black circle represent the core whereas the dashed circle represent the surface of the shell. Some of the polyelectrolyte chains is depicted in the shell. **A:** a counterion condensed on the polyion, **B:** a counterion free to move within the shell and **C:** a counterion which can leave the shell.

shell [Das et al., 2002]. Furthermore the osmotic coefficient of these colloidal suspensions are independent of polymer concentration i.e. the fraction of free counterions are constant [Das et al., 2002].

When the polyelectrolyte chains are anchored close enough on the core, the distance between the chains is smaller than the local screening length and hence the distribution of counterions is only depend on the distance from the core [Dubreuil and Guenoun, 2001]. The radial distribution of counterion resembles the distribution of monomeric units of the polyelectrolyte [Dubreuil and Guenoun, 2001, Dingenouts et al., 2004].

5. Experimental approach

As mentioned in chapter 3 on page 11 the PS-PAA samples will be investigated both in their protonated and in their deprotonated form to study the contribution to the water activity from the charges and the counterions. It is chosen to focus on sodium as counterion i.e. all measurements will be performed on samples containing sodium as counterion unless the sample is in the protonated form. In order to achieve PS-PAA particles with deprotonated acid groups (denoted PS-NaPAA) pH in the PS-PAA suspension will be increased to pH 9.5, which is determined to be the equivalence point [Nielsen, 2009] for the particles in a 0.1 M NaClO₄ solution.

To be able to correlate the measured water activity to the different parts of the PS-NaPAA particles, substances resembling the different parts of the particles are measured individually. Hence bare polystyrene (PS) particles, free sodium polyacrylate (NaPAA) and sodium acrylate (abbreviated NaAc) will be measured in the same concentration range. The free sodium polyacrylate will be obtained by adjusting pH to 9.5 in solutions of PAA. Since there is evidence that the water activity of some polymer solutions depends on the molecular weight of the polymer [Money, 1989], the size of the free PAA must be chosen to correspond to the size of the PAA in the shell. Hence the size of the PAA shell must be determined. According to [Christensen, 2008] the PAA chains is fully stretched above pH 9.3 and completely collapsed at pH 3. Thus the size of the PAA chain will be determined by measuring the size at pH 9.5 and pH 3. The size of the particles will be determined by dynamic light scattering as this method is well suited for determination of the size of polyelectrolyte core-shell particles [Guo and Ballauff, 2001]. The procedure for calculating the size of the chains can be found in appendix A.2. The size determined in this manner corresponds to the size of the longest PAA chains [Guo and Ballauff, 2001]. The water activity will be measured using a chilled-mirror dewpoint method as this method is comparable simple and can be used in a large concentration range [Decagon Devices, Inc, 2008].

To be able to measure the water activity for concentrated samples, the suspensions/solutions will be freeze-dried. Freeze-drying is chosen to concentrate the samples as preliminary experiments show that freeze-drying do not damage the samples (cf. appendix B on page 77). The concentration of the samples will be stepwise decreased by addition of water. The samples will not be stirred after addition of water as preliminary experiments (not shown) showed that stirring result in sample loss.

The concentrations of the samples will be calculated according to the dry matter content in suspensions before freeze-drying. After each experiment the dry matter content will be

determined to measure the sample loss during the experiments.

To be able to fit the model by Filho and Maurer [2008] the limiting osmotic coefficient must be obtained. Hence diluted suspensions of PS-NaPAA will be measured using membrane osmometry, since membrane osmometry can measure the osmotic pressure for samples to dilute to be measured using the chilled-mirror dewpoint method.

Besides the measurements of water activity as a function of water content (i.e. gram water per gram dry matter, denoted Y), the water activity for PS-NaPAA is also studied as a function of temperature to be able to calculate the excess enthalpy for water associated with the PS-NaPAA particles as described in section 4.3.3 on page 21. In order to keep the water content constant in a series of measurements the water activity at different temperatures are measured in continuation of each other without any interruption.

Since the relative humidity (RH) of the laboratory may cause water uptake or evaporation from the samples, the relative humidity in the laboratory will be measured.

For comparison a sample of PS-NaPAA will be measured using simultaneous thermal analysis (STA) to dry a sample at constant temperature. The flux in mass loss can be obtained from this measurement and as the flux is proportional to the water vapor pressure above the sample these measurements can be compared to the water activity measured as a function of water content. Additionally the energy needed to evaporate the water from the PS-NaPAA suspension can be compared with the excess enthalpy determined from the measurements of water activity as a function of temperature.

Thus the particles will be initially characterised to obtain the size of the particles and the dry matter content. The water activity for the PS-NaPAA will be measured both as a function of water content and as a function of temperature. The measured water activity as a function of water content will be fitted with both the model by Filho and Maurer [2008] and with the BET isotherm as these may describe different parts of the concentration range. Additionally samples of PS-PAA, NaAc, PS and NaPAA will be measured as a function of water content to be able to interpret which part of the PS-NaPAA particles that has the largest impact on the water activity. Finally the PS-NaPAA suspension will be dried using STA.

6. Methods

The suspensions of PS-PAA particles studied in this project is synthesised by free-radical surfactant-free emulsion polymerisation using a procedure similar to the procedure described by [Hinge, 2006]. Though the synthesis is performed without extra salt and the acrylic acid is added after 1 hour of styrene polymerisation. After synthesis the PS-PAA is purified by dialysis.

Suspensions of bare PS particles is produced by the same procedure as the PS-PAA suspension by omitting the addition of acrylic acid¹.

6.1 Determination of dry matter content

The dry matter content in the suspensions of PS-PAA is determined in triplicate according to [DS 204, 1980]. Aluminum weigh dished are dried in an oven (Model UE 200, Memmert, Germany) at 105 °C in an hour. The weigh dishes are cooled in a desiccator and weighed (Mettler AM100, Switzerland). Each dish is added 3 ml of the PS-PAA suspension (shaken). The dishes with PS-PAA is dried in a 105 °C oven for at least 20 hours, cooled in a desiccator and weighed.

Dry matter content for the suspension of bare PS particles is determined using the same procedure. Additionally the dry matter content of PAA (M_w approx. 2000, Aldrich, Germany) is determined according to the described procedure with the exception that the dry aluminum dish containing the PAA is weighed before drying as well.

6.2 Size determination by dynamic light scattering

In order to calculate the size of the shell, the size of the PS-PAA particles is measured by dynamic light scattering.

A stock suspension of 5 μ l PS-PAA particle suspension and 25 ml demineralised water is prepared. A part of the stock solution is adjusted to pH 3 (PHM200 MeterLabTM, Radiometer, Denmark. pH electrode 11, Schott Instruments, Germany) with HCl (Sigma-Aldrich >37 %, Germany) and the remaining stock suspension is adjusted to pH \approx 9.5 with NaOH (>99 %, Merck, Germany) before measuring the size by dynamic light scattering (Zetamaster, Malvern Instruments, United Kingdom). Each suspension is measured twice and each of the measurements consists of three sub-measurements. The reported size is

¹The dialysed PS-PAA and PS suspensions is kindly supplied by Jonas Laursen

an average of all six sub-measurements. For each sub-measurement the number average size is used. After the size measurement the pH is measured again.

The bare PS particles are measured using the same procedure except that the size is measured without any adjustment of pH.

6.3 Determination of water activity

6.3.1 Sample preparation

The PS-PAA particles in the stock suspension are in their protonated form. To achieve samples with PS-PAA in deprotonated form pH is increased to pH 9.5 with sodium hydroxide.

The PS-PAA, PS-NaPAA and the PS particles is freeze-dried by transferring 8 ml of the given suspension to a pre-weighed (Mettler AM100, Switzerland) sample cup (Decagon Devices, Inc, USA) which is closed with a pre-weighed lid (Decagon Devices, Inc, USA) with air holes. The suspension is frozen in the sample cup before it is freeze-dried (Christ Alpha 1-2 LDplus, Germany). After drying, the lid with air holes is immediately covered with a pre-weighed piece of parafilm[®] (Pechiney plastic packing, USA).

Samples of free NaPAA is prepared by dissolving an appropriate amount of PAA in demineralised water and adjusting to pH 9.5. The samples are freeze-dried using the procedure described above with the exception that the volume of the NaPAA solution is adjusted to reached a total dry matter content of 0.3 - 0.35 g.

Sodium acrylate (97 %, Aldrich, USA) is used as received.

6.3.2 Water activity as a function of water content

The water activity of the samples are measured using Aqualab (Aqualab 4TE Decagon Devices, USA) at a pre-set temperature (30 or 40 °C). The samples is measured numerous times until three subsequent measurements differ by less than 0.0005. At this point no significant change in water activity is assumed to take place. The sample cup is removed from the Aqualab, closed and weighed immediately to obtain the water content (g water per g solid) corresponding to the measured water activity.

A small amount of demineralised water (at least 5 μ l) is added to the sample before a new measurement is started. The amount of water added before each measurement is gradually increased as the water activity increases. When more than 5 μ l water is added the water is added in portion to different parts of the sample to get are better initial distribution of the water.

This procedure is repeated until a_w equals 1. When such measurement series are longer than one day the sample is covered with the lid and placed in the laboratory overnight as preliminary results show no change in water activity due to storage (cf. appendix C on page 80).

After each measurement series the sample cup containing the sample and the lid is dried for at least 20 h in an oven at 105 °C and subsequently weighed to verify the initial calculated dry matter content. All measurement series is conducted twice except for PS. At least once a day the relative humidity in the laboratory is measured using a capacitive humidity sensor (Honeywell HIH-4000-001, Mexico).

6.3.2.1 Validation of method

To verify the procedure described in section 6.3.2 a sample of PS-NaPAA at pH 9.5 is freeze-dried. Demineralised water is added until $a_w \approx 0.75$ and the water activity of the sample is measured at 30 °C using Aqualab several times over a period of 19 days. Between the measurements the sample is stored in a closed sample cup at room temperature (approximately 22 °C).

6.3.3 Water activity as a function of temperature

A sample of PS-NaPAA at pH 9.5 is freeze-dried in a pre-weighed measurement cup with a lid with air holes. After freeze-drying the lid is closed with parafilm. The sample is weighed and the water activity is measured using Aqualab. The sample is measured in the temperature interval 20-50 °C starting at 20 °C and increasing the temperature in steps of 5 °C when three subsequent measurements differ by less than 0.0005. After reaching a stable water activity at 50 °C the sample is weighed and demineralised water is added. After weighing the sample the water activity is measured once again in the same temperature range by repeating the described procedure. After finishing the measurement series the sample cup and lid are oven-dried at 105 °C for at least 20 hours and weighed.

6.4 Osmotic pressure by membrane osmometry

The stock suspension of PS-PAA is adjusted to pH 9.5 with sodium hydroxide. Afterwards the suspension is diluted and the dilutions are adjusted to pH 9.5 with the stock suspension of PS-PAA. The osmotic pressure of the resulting suspensions is measured using membrane osmometry (Osmomat 90, Gonotec Berlin, MWCO 20 kD). 0.6 ml of the investigated suspension is repeatably injected into the membrane osmometer until the response for the

pressure difference across the membrane is constant. The measurements is corrected for the pressure difference across the membrane before and after measuring the suspensions by injection of demineralised water until a stable value for the pressure response is obtained.

6.5 Drying by simultaneous thermal analysis

5 ml of the stock suspension of PS-PAA was adjusted to approximately pH 9.5 by use of sodium hydroxide. The suspension is centrifuged in 20 minutes at 20 °C with a speed of 15000 rpm (Eppendorf Centrifuge 5403, Germany). The supernatant is removed and the pellet is used for measuring by simultaneous thermal analysis (STA) (Netzsch STA 449 C, Jupiter, Germany). Approximately 40 mg of the concentrated PS-NaPAA sample is transferred to a pre-weigh aluminium crucible and weighed. The crucible is placed in the STA and dried at 40 °C under an air flow of 40 ml/min. The samples are measured with 240 measurement points per min.

From the measured mass loss the flux is calculated by numeric differentiation over 400 points. The energy input from STA is converted to a quantity proportional to the enthalpy by dividing the energy input with the calculated flux.

7. Results

In this chapter the results are presented. The different samples are denoted with the the abbreviation for the substance followed by the temperature at which the sample is measured and a number indicating if it is the first or the second measurements series for the given substance at the given temperature. Thus PS-NaPAA-30-1 is the first sample of PS-NaPAA at 30 °C. For the samples measured by membrane osmometry the same notation is used except a M is added before the number of the measurement e.g. PS-NaPAA-30-M1. For the samples measured at different temperatures a T is used instead of the temperature e.g. PS-NaPAA-T-1.

7.1 Initial characterisation of the particles

Table 7.1 shows some characteristics for the PS-PAA and the PS particles. The dry matter content is determined as described in section 6.1 and the charge density (σ , charges per gram dry matter) is taken from [Nielsen, 2009]. The size of the particles is measured as described in section 6.2 on page 27. During the measurements at pH 9.5, pH decreased slightly but no tendency between the decrease in pH and the determined size was observed. The remaining values given in table 7.1 are calculated according to appendix A on page 73 from the dry matter content, σ and the size.

Table 7.1: Selected characteristics for the PS-PAA and PS particles. σ denotes the charges per gram drymatter, r_{col} and r_{swol} denotes the radius of the collapsed and the swollen particle respectively, r_{core} is the radius of the core, M_{PAA} is the maximum molecular weight of each PAA chain in the shell, c_p is the concentration of particles, and z_p is the number of charges per particle. The values are calculated according to appendix A on page 73. *[Nielsen, 2009].

	PS-PAA	PS
Dry matter [g/L]	24.4±0.1	30.49±0.04
* σ [meq/g]	2.4±0.05	
r_{col} [nm]	114	
r_{swol} [nm]	158	
r_{core} [nm]	105	190
M_{PAA} [kg/mol]	15	
c_p [particles/L]	$3.50 \cdot 10^{15}$	$1.02 \cdot 10^{15}$
z_p	$1.01 \cdot 10^7$	$8.97 \cdot 10^5$

The size of the PS particles is observed to be almost twice as large as the size of the PS core in the PS-PAA particles. The molecular weight of each PAA chain in the shell is

observed to be approximately 7.5 times larger than the molecular weight of the free PAA used for comparison.

From the size of the PS-PAA particles the water content necessary to fill the shell of the particles with water can be calculated according to appendix A.4. The resulting values is given in table 7.2.

Table 7.2: The water content needed to swell all particles in the given sample along with the corresponding x_w .

Sample	Y_{shell}	$x_{w,shell}$
PS-NaPAA-30-1	1.59	0.98
PS-NaPAA-30-2	1.60	0.98
PS-NaPAA-40-1	1.57	0.97
PS-NaPAA-40-2	1.60	0.98
PS-NaPAA-T-1	1.42	0.97
PS-NaPAA-T-2	1.42	0.97
PS-NaPAA-T-3	1.42	0.97
PS-NaPAA-T-4	1.40	0.97

For all PS-NaPAA particles x_w for one hydration layer (4 water molecules per sodium ion [Cotton et al., 1995]) on each sodium ion is $x_w = 0.80$ where as complete hydration (16.6 water molecules per sodium ion [Cotton et al., 1995]) of all sodium ions correspond to $x_w = 0.94$. The corresponding values for NaPAA-30-1 is $x_w = 0.78$ and $x_w = 0.94$ and for NaPAA-30-2 $x_w = 0.79$ and $x_w = 0.94$.

The charge density parameter is calculated by equation 4.6 on page 15 to be 2.33 at 30 °C (ϵ_r is taken from [Fernandez et al., 1995]).

7.2 Water activity as a function of water content

The water activity for samples of PS-NaPAA, PS, PS-PAA, NaPAA, and NaAc was measured as a function of water content by the method described in section 6.3.2 on page 28. In order to validate this method, the water activity for a sample of PS-NaPAA was measured repeatably over a period of 19 days as described in section 6.3.2.1. The results for these measurements is presented in the following section.

7.2.1 Validation of method

To validate the method for measuring the water activity described in section 6.3.2, a_w was measured repeatably in a PS-NaPAA sample over a period of 19 days. a_w measured in this period and the corresponding water content is shown in figure 7.1 as function of

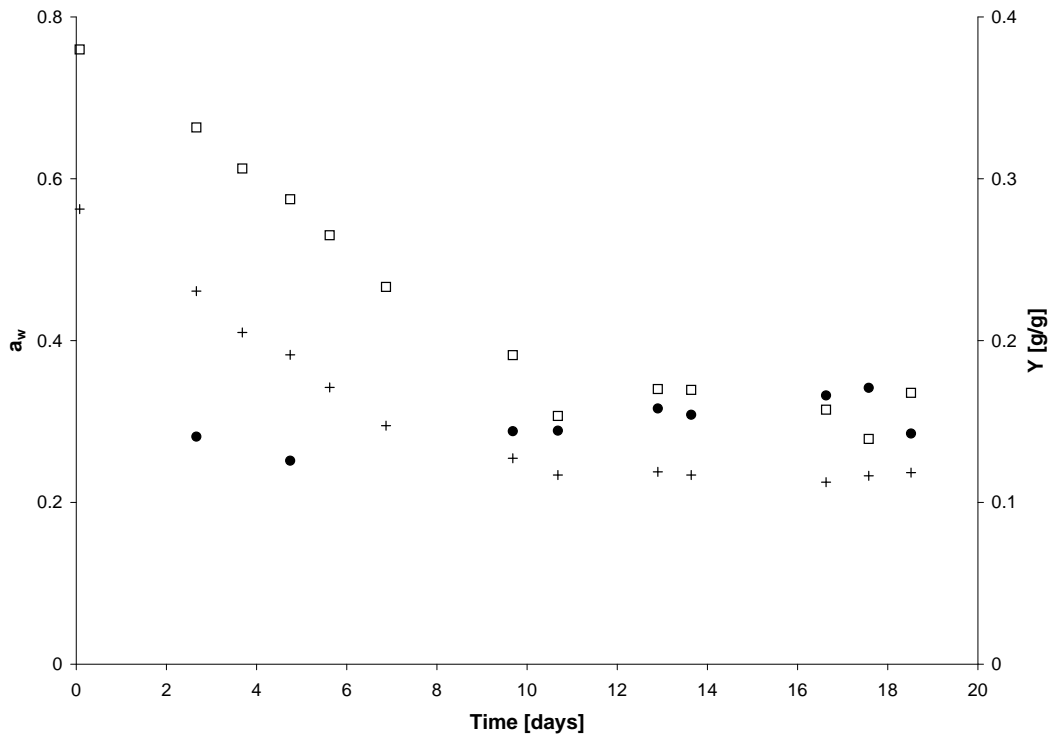


Figure 7.1: The water activity (□), water content (+), and the relative humidity of surroundings (•) as a function of time.

time along with the relative humidity of the surroundings.

The fall in water activity measured during the first 10 days is due to the evaporation of water from the sample. After 10 days the water activity cease at approximately $a_w = 0.3$, which corresponds to the relative humidity in the laboratory. In the period from day 10 until day 19 no distinct tendency is observed in the water activity, hence equilibrium may be established in the sample. The measured a_w may not be the true equilibrium water activity, since the sample is stored at a lower temperature between the measurements, than the measurement temperature, thus a new equilibrium must first be established during the measurement. The variation in the water activity measurements is not observed to depend on the variation of the relative humidity of the surroundings.

In figure 7.2 the water activity from the above mentioned experiment is plotted against Y and compared to the water activity measured for two samples at 30 °C measured according to section 6.3.2 on page 28.

For the measurement series measured over a period of 19 days the highest value for a_w is obtained at day 1. The approximately constant water activity observed in figure 7.1 is observed at $Y = 0.12$ in figure 7.2. According to figure 7.2 the water activity measured over a period of 19 days differs more and more from the water activity measured in the ordinary way as equilibrium is established in the sample cup. Hence equilibrium may not

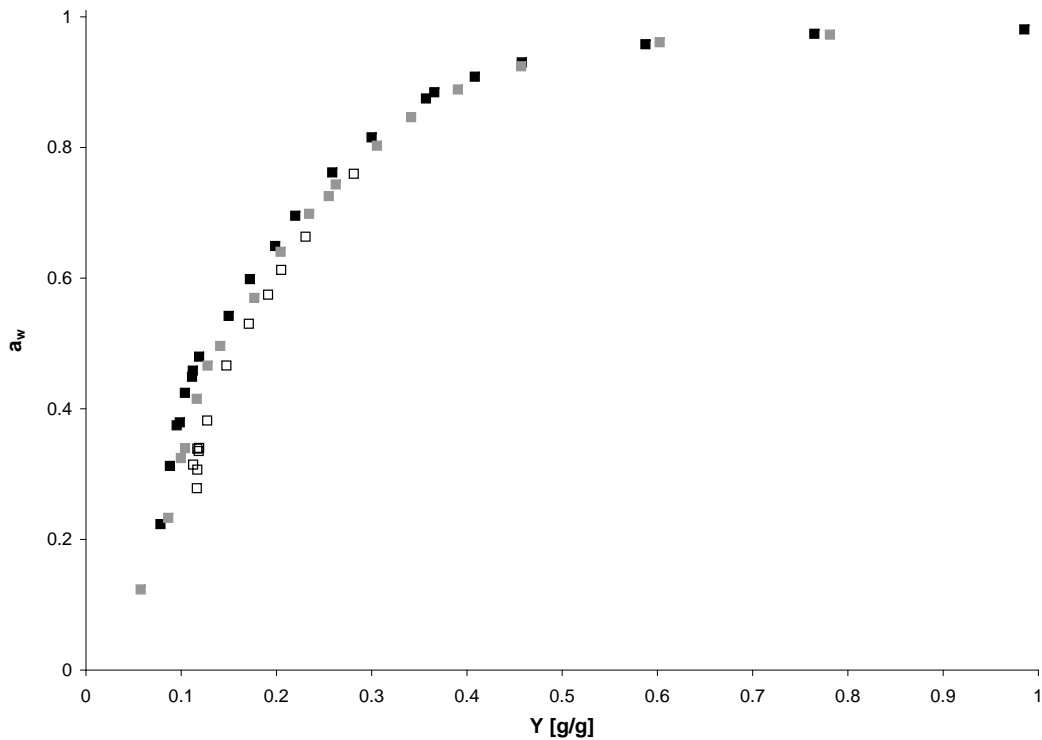


Figure 7.2: The water activity (■ and ■) measured as described in section 6.3.2 as a function of water content and the water activity (□) measured over a period of 19 days as a function of water content. The highest value for a_w is obtained of the first day of measurement after which a_w decreases.

be established in the two ordinary measurements series. As seen in figure 7.2 the two measurements series without long equilibration time are slightly different as well. This difference may depend on how far from equilibrium the measurement is performed. As the measurements is most likely not at equilibrium, the measurements may not be accurate, but since the a_w vs. Y tendency is reproduced for all three measurement series depicted in figure 7.2 the measurements is assumed to reflect the reality.

When using the method described in 6.3.2 the amount of water added to the samples is observed to be larger than the amount of water calculated from the weighing. This means that water is evaporating from the samples.

In table 7.3 the relative humidity in the laboratory on the day of measurements is given along with the percentage of the total amount of evaporated water which is assumed to evaporate inside Aqualab. This amount of water is calculated by assuming that all the water necessary to reach the measured water activities is evaporated from the sample i.e. the water activity of the air in Aqualab is zero until water is evaporated from the sample. Additionally the water vapour is assumed to behave ideally.

According to table 7.3 less than 25 % of the evaporated water can be ascribed to equilibration of the sample and the air in Aqualab. Thus water must evaporate somewhere

Table 7.3: The range for the relative humidity [%] in the laboratory on the days of measurements for the given samples.

Sample	Lowest RH [%]	Highest RH[%]	% evap. water theoretical
PS-NaPAA-30-1	18±3.5	25±3.5	17.1
PS-NaPAA-30-2	22±3.5	25±3.5	10.6
PS-NaPAA-40-1	31±3.5	39±3.5	13.4
PS-NaPAA-40-2	29±3.5	35±3.5	14.5
PS-30	29±3.5	32±3.5	-10.3
PS-PAA-30-1	34±3.5	40±3.5	8.7
PS-PAA-30-2	32±3.5	40±3.5	23.7
NaPAA-30-1	21±3.5	27±3.5	6.8
NaPAA-30-2	27±3.5	29±3.5	18.4
NaAc-30-1	31±3.5	43±3.5	11.3
NaAc-30-2	32±3.5	36±3.5	18.7

else in the procedure. No correlation between the theoretical evaporated amount of water and the relative humidity in the laboratory is found. It is assumed that the water content calculated from the weighing represent the actual water content in the samples. The negative value for PS-30 in table 7.3 is due to sample loss during measurement as will be described later.

As described in this section the method described in section 6.3.2 may not give accurate values for a_w but the measurements obtain by this method is assumed to reflect the reality. Hence the results obtained by this method for PS-NaPAA, PS, PS-PAA, NaPAA and NaAc are presented in the following sections.

7.2.2 Poly(styrene-*co*-sodium acrylate) particles

Samples of PS-NaPAA was measured as a function of water content at both 30 and 40 °C. The observations and results are presented in the following.

Table 7.4 shows the degree of charge neutralisation in the samples of PS-NaPAA. The degree of neutralisation is calculated as the amount of sodium hydroxide divided by the amount of acrylic acid groups present in the samples.

Table 7.4: The degree of neutralisation for the samples of PS-NaPAA.

Sample	Degree of neutralisation
PS-NaPAA-30-1	0.998
PS-NaPAA-30-2	0.991
PS-NaPAA-40-1	1.016
PS-NaPAA-40-2	0.963

As can be seen from table 7.4 all samples of PS-NaPAA is approximately neutralised.

The freeze-dried samples of PS-NaPAA is a fluffy substance which is fixed to the bottom of the sample cup as seen in figure 7.3*left*. Hence a minimum of sample is lost during the measurement series. The conversion of sample dry matter content is confirmed by the weigh after the the final drying of the samples, which deviates by less than 3.5 % from the amount calculated from the known amount of PS-NaPAA in the suspension before freeze-drying. The fluffy sample structure collapses gradually when water is added to the



Figure 7.3: *Left:* A sample of PS-NaPAA after freeze-drying. *Right:* A sample of PS-NaPAA after freeze-drying and water addition. The holes in the sample correspond to the places where a drop of water has been added.

sample. The sample collapses completely at the specific site of water addition as seen in figure 7.3*right*, whereas the remaining part of the sample is observed to collapse more slowly as the water content is increased.

The water activity as a function of water content (Y) for the four samples of PS-NaPAA is shown in figure 7.4. At higher water content than the range shown in figure 7.4 a_w approaches 1 and hence this part is omitted from figure 7.4 to give a better view of the range in which a_w is changing significantly.

According to figure 7.4 a_w for the samples change in the same manner with increased water content. The samples generally have a steep increase until $Y \approx 0.11$. Above $Y \approx 0.11$ a_w increases less and less with increases water content. Figure 7.4 shows no significant difference between the measurements at 30 and 40 °C except in the range $0.3 < Y < 0.8$ where PS-NaPAA-40-1 is slightly lower than the three others. Since this tendency is not reproduced for PS-NaPAA-40-2, no clear tendency by varying the temperature is observed and hence the remaining samples are only measured at 30 °C.

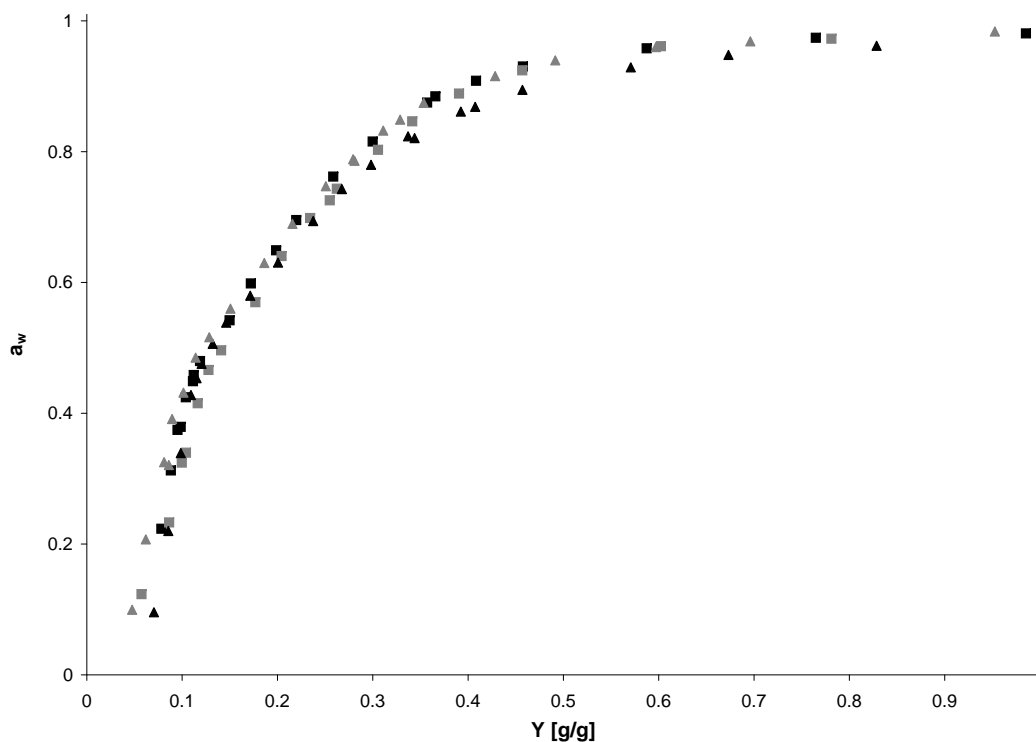


Figure 7.4: The water activity as a function of water content for PS-NaPAA-30-1 (■), PA-NaPAA-30-2 (■), PS-NaPAA-40-1 (▲), PS-NaPAA-40-2 (▲).

7.2.3 Bare polystyrene particles

The water activity was measured as a function of water content for one sample of PS particles using the procedure described in section 6.3.2.

The freeze-dried PS is loose particles which do not stick to the sample cup as was the case for PS-NaPAA. Hence a part of the PS sample was observed to be lost before, during and after the measurement series. Figure 7.5 shows the water activity as a function of the water content. As some of the sample is lost during the measurement series the measured a_w is plotted as a function of both the water content calculated according to the dry matter content of the PS suspension and the water content based on the final dry matter content. According to the weighting 13.3 % of the sample dry matter content is lost during the measurement series.

According to figure 7.5 the water activity of PS increase to $a_w = 1$ with in a very small water content range. Since the water content based on the initial dry matter content is calculated to be negative it is evident that sample is lost already before the measurement series is started. The behaviour of the first three points is believed to be due to sample loss as well. Taken the sample loss into account the water activity is assumed to increase steeply towards $a_w = 1$ at $Y \approx 0$. Hence PS particles have no influence on the water

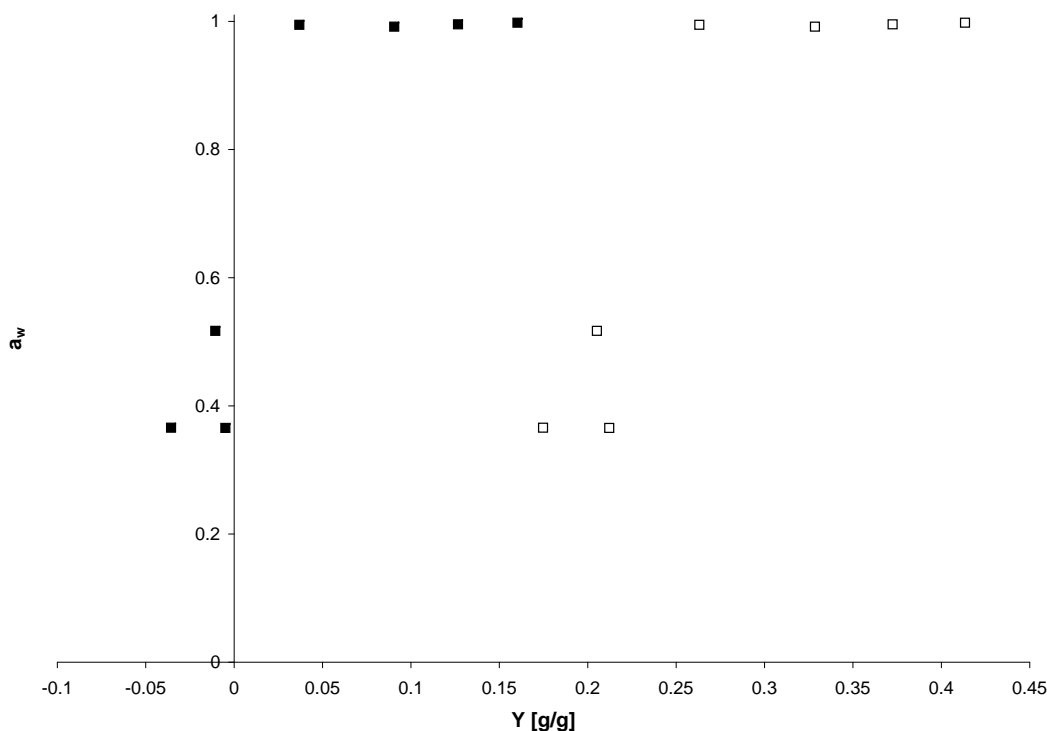


Figure 7.5: The water activity as a function of water content for PS-30-1. The water content is calculated from the initial dry matter content (■) and according to the final dry matter content (□).

activity. This is confirmed by the fact that the PS particles is observed to repel the water added to the sample.

7.2.4 Poly(styrene-*co*-acrylic acid) particles

In order to determine the charges and the counterions impact on the water activity samples of PS-PAA is measured as a function of water content. The samples of PS-PAA is assumed to be completely protonised.

The freeze-dried samples look similar to the freeze-dried PS-NaPAA. The final determination of the dry matter content deviates by less than 1 % from the initial dry matter content. The measurement for a_w as a function of water content is depicted in figure 7.6. According to figure 7.6 a_w increases steeply at low water content but above $Y \approx 0.05$ the water activity increases gradually less and less with increasing water content. The two measurements series progress similar except for the lowest measured a_w for PS-PAA-30-1 which is measured at higher water content than the following a_w . No explanation for this behaviour is found and hence it is assumed to be a experimental error.

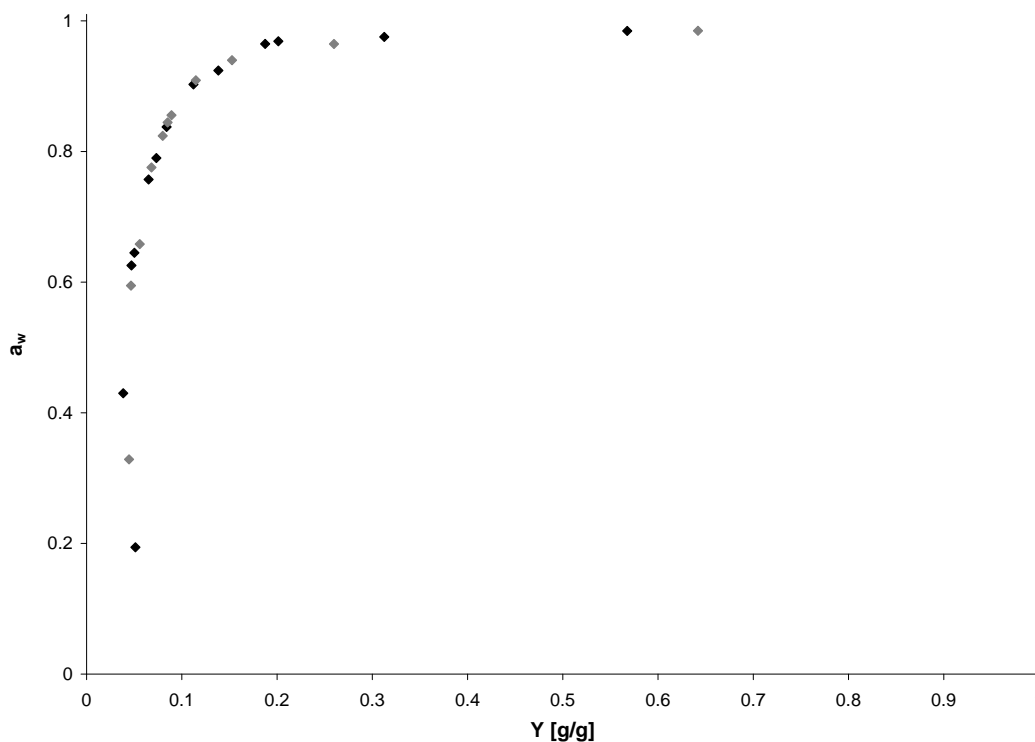


Figure 7.6: The water activity as a function of water content for PS-PAA-30-1 (◆) and PS-PAA-30-2 (◆).

7.2.5 Sodium polyacrylate

Two samples of PAA ($M_w = 2$ kD) was neutralised with sodium hydroxide and measured according to the method in section 6.3.2. The degree of neutralisation of PAA in the NaPAA samples is given in table 7.5. It is noted that the NaPAA is only partly neutralised.

Table 7.5: The degree of neutralisation for the samples of NaPAA.

Sample	Degree of neutralisation
NaPAA-30-1	0.766
NaPAA-30-2	0.795

The freeze-dried samples of NaPAA appear as a glassy network which is partly fixed to the bottom of the sample cup. According to the initial and final dry matter content approximately 4 % of the sample is lost during both of the measurement series. The water activity as a function of the water content is depicted in figure 7.7 along with values from the literature.

According to figure 7.7 the measured water activity increases with increasing water content. For both NaPAA-30-1 and NaPAA-30-2 the water activity increases most steeply until $Y \approx 0.3$. Above $Y \approx 0.3$ a_w increases less with increased water content. The water activity do not reach one before $Y \approx 15$ (not shown in figure 7.7). The water activity as a

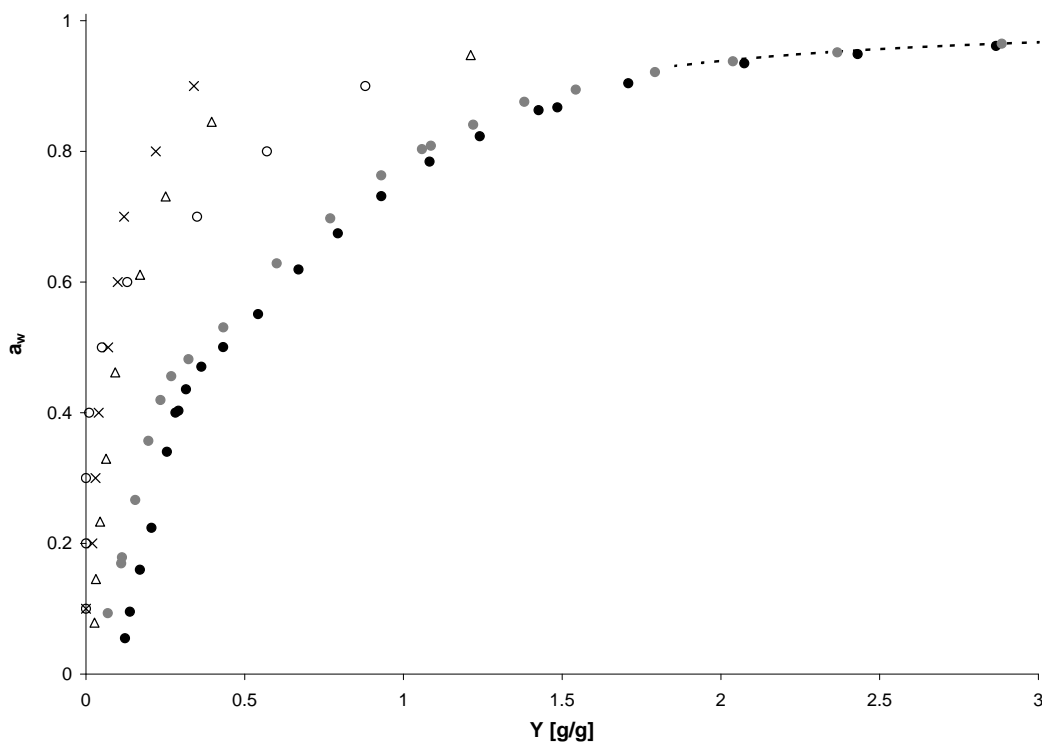


Figure 7.7: The water activity as a function of water content for NaPAA-30-1 (●) and NaPAA-30-2 (●) $M_w = 2$ kD. Additionally literature data is shown for PAA 1250 kD (Δ) [Hwang et al., 1998], PAA $M_n=1.8$ kD (\times) and NaPAA $<1000 \mu\text{m}$ (\circ) [Thijs et al., 2007] along with the model for NaPAA $M_n=2.6$ kD obtained from [Filho and Maurer, 2008] (---).

function of the water content for NaPAA-30-2 deviates from the corresponding measurements for NaPAA-30-1. The deviation is most pronounced below $a_w \approx 0.45$.

In general the water activity from the literature is above the values obtained in this project. The model by Filho is observed to correspond to the measured a_w . The model by Filho and Maurer is only included in the range where Filho and Maurer has fitted the model to their measurements.

7.2.6 Sodium acrylate

Two samples of sodium acrylate was measured as a function of water content.

The sodium acrylate is a white powder which was measured without any initial drying. No sample loss were observed during the measurement series. This is confirmed by the final dry matter content determination which differ by less than 2 % from the initial weighing. In the beginning of the two measurement series the water added to the samples stay as the drops at the surface of the sodium acrylate. If these drops are still visible when a stable a_w is obtained, the sample is measured again and only the measurements, where

no distinct drops was observed in the sample after the measurement, is used. Figure 7.8 shows the measured a_w as a function of water content.

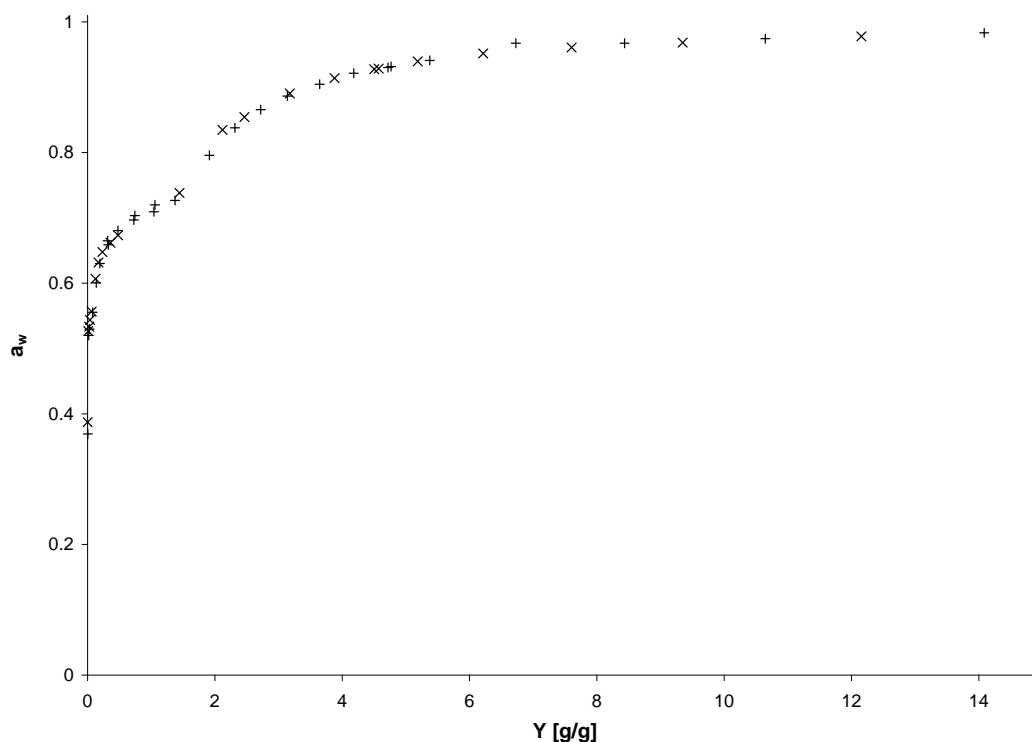


Figure 7.8: The water activity as a function of water content for NaAc-30-1 (\times) and NaAc-30-2 ($+$).

As depicted in figure 7.8 the water activity as a function of water content is reproducible for NaAc. According to the figure the water activity increases stepwise. The water activity increase gradually less and less with increasing water content until $a_w \approx 0.73$ i.e. $Y \approx 1.4$. Above $Y \approx 1.4$ the water activity increases steeply and then increase asymptotic towards $a_w = 1$. For both samples the measurement at $Y \approx 1.4$ is observed to be the last point where some of the sodium acrylate is not dissolved. Thus the plateau at $a_w \approx 0.73$ may corresponds to the water activity of a saturated NaAc solution.

7.2.7 Comparison of water activity for the parts of PS-NaPAA

To determine which parts of the PS-NaPAA that influence the water activity, the water activities given above for PS-NaPAA, PS, PS-PAA, NaPAA and NaAc are compared. As mentioned in section 7.2.3 the PS particles has no influence on the measured water activity.

Figure 7.9 shows the water activity as a function of water content for PS-NaPAA-30-2 and PS-PAA-30-2. This samples is representative for PS-NaPAA and PS-PAA respectively.

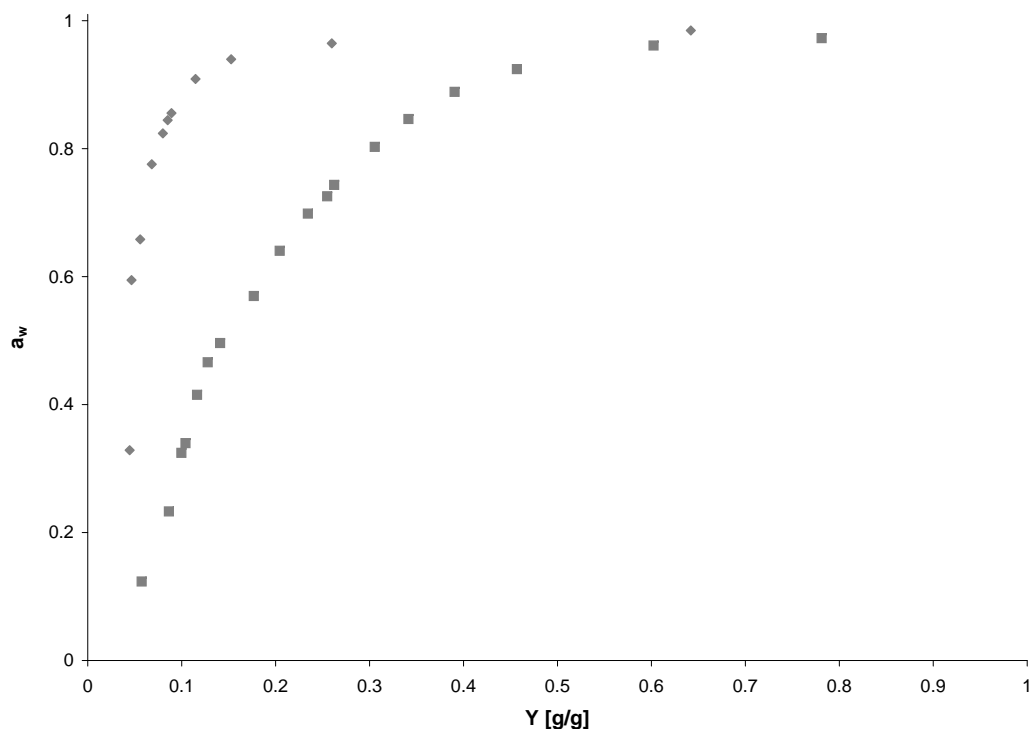


Figure 7.9: The water activity as a function of the water content for PS-NaPAA-30-2 (■) and PS-PAA-30-2 (◆).

Figure 7.9 shows that the water activity is considerably lower for PS-NaPAA than for PS-PAA at the same water content.

A comparison of PS-NaPAA-30-2 with NaAc-30-1 and NaPAA-30-1 is shown in figure 7.10. These samples are representative for the different types of samples. To compare the different samples the water activity is plotted against the modified mole fraction of water (x_w^*). x_w^* is calculated regarding only the sodium ions and the water in the samples. The advantage of using x_w^* to compare the PS-NaPAA with NaPAA and NaAc is that at the same mole fraction of water PS-NaPAA, NaPAA and NaAc contains the same amount of sodium ions and hence the same amount of charges carboxylate groups (neglecting counterion condensation).

According to figure 7.10 PS-NaPAA and NaPAA approach each other with increased mole fraction of water until $x_w^* \approx 0.9$. PS-NaPAA has a lower water activity than NaPAA until $x_w^* \approx 0.9$ after which a_w for NaPAA and PS-NaPAA is approximately equal.

The water activity for NaAc approach PS-NaPAA above $x_w^* \approx 0.78$ which is the point at which all NaAc is dissolved. Above $x_w^* \approx 0.9$ the water activity for NaAc resemble the water activity for NaPAA and PS-NaPAA.

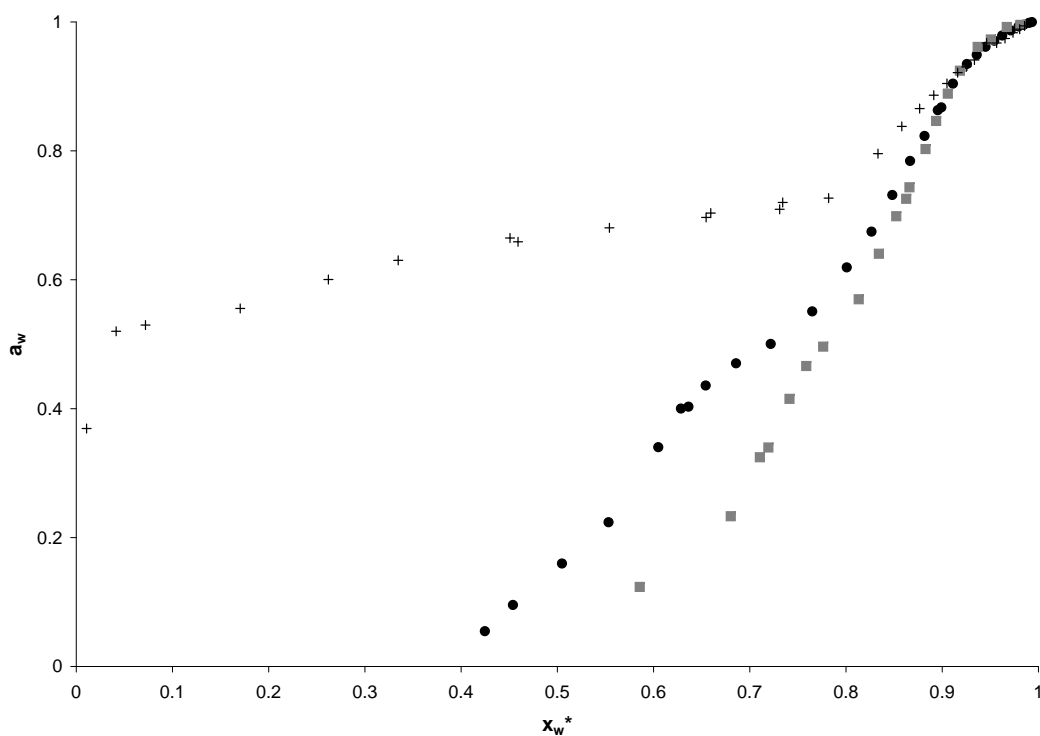


Figure 7.10: The water activity as a function of the modified mole fraction of water (see text) for PS-NaPAA-30-2 (■), NaPAA-30-1 (●) and NaAc-30-2 (+).

As noted the water activity as a function of the water content has a bend for all samples of PS-NaPAA and NaPAA. The values for the measurement closest to the bend are listed in table 7.6.

Table 7.6: The modified mole fraction of water corresponding to the bend on the plots of a_w as function of water content.

Sample	x_w^{*bend}
PS-NaPAA-30-1	0.718
PS-NaPAA-30-2	0.759
PS-NaPAA-40-1	0.743
PS-NaPAA-40-2	0.743
NaPAA-30-1	0.654
NaPAA-30-2	0.611

According to table 7.6 x_w^{*bend} is approximately the same for all PS-NaPAA samples. The small differences in the values of x_w^{*bend} are assumed to be due to the fact that only discrete points for a_w is present and hence the number of measurements just around the bend is determining for the exact values for x_w^{*bend} . The x_w^{*bend} for NaPAA is approximately the same for the two samples, but lower than for PS-NaPAA.

7.2.8 Comparison of activity coefficient for water

As mentioned in section 4 on page 13 the water activity consist of a colligative term (x_w) and a term describing the interaction between the solutes and the water (γ_w). Since the colligative part of a_w is not equal for e.g. the samples of PS-NaPAA and NaAc γ_w for the different samples is compared to examine the difference between the samples interactions with water. γ_w is calculated according to equation 4.1. In figure 7.11 γ_w for PS-NaPAA-30-2, NaPAA-30-1, PS-PAA-30-2 and NaAc-30-2 is given as a function of x_w . Note that for PS-NaPAA $x_w = x_w^*$.

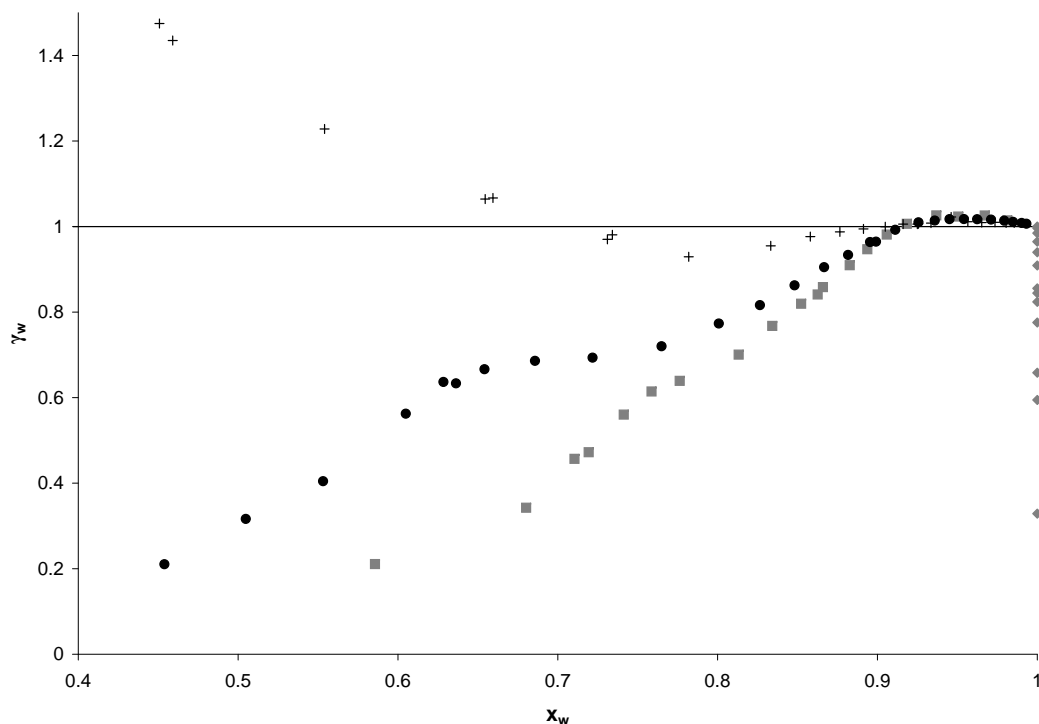


Figure 7.11: The activity coefficient for water as a function of x_w for PS-NaPAA-30-2 (■), PS-PAA-30-2 (◆), NaAc-30-2 (+) and NaPAA-30-1 (●).

In general γ_w is observed to increase with increasing x_w for PS-NaPAA-30-2 and NaPAA-30-1. At $x_w \approx 0.9$ γ_w increase beyond one. Above $x_w \approx 0.95$ γ_w decreases towards one. For NaAc-30-2 γ_w decreases until $x_w \approx 0.78$. The decrease is observed outside the range of figure 7.11 as well. Above $x_w \approx 0.78$ γ_w for NaAc-30-2 approach the behaviour of the values for PS-NaPAA-30-2 and NaPAA-30-1. Since no counterions is present in samples of PS-PAA, $x_w \approx 1$ for all measurements and hence γ_w is observed to increase towards one very close to $x_w = 1$.

The bends observed for PS-NaPAA-30-2 and NaPAA-30-1 in the range $0.6 < Y < 0.85$ in figure 7.11 corresponds to the bend in a_w as a function of the water content as described above.

The behavior of γ_w described above is representative for the behaviour of all investigated sample. The x_w at which γ_w increase above one is given for all samples in table 7.7. Since only discrete measurements is available the intersection is given by the last value of x_w for which $\gamma_w < 1$ and the first x_w for which $\gamma_w > 1$.

Table 7.7: The lower and upper limit for $\gamma_w = 1$.

Sample	x_w lower	x_w higher
PS-NaPAA-30-1	0.91	0.92
PS-NaPAA-30-2	0.91	0.92
PS-NaPAA-40-1	0.93	0.94
PS-NaPAA-40-2	0.92	0.93
NaPAA-30-1	0.91	0.93
NaPAA-30-2	0.90	0.91
NaAc-30-1	0.89	0.91
NaAc-30-2	0.91	0.92

As seen in table 7.7 the intersection for $\gamma_w = 1$ is approximately constant for the different samples of PS-NaPAA, NaPAA and NaAc. The slightly higher values for PS-NaPAA-40-1 is caused by the slightly lower a_w measured for PS-NaPAA-40-1 in this range than for the remaining PS-NaPAA samples.

7.2.9 Modelling the osmotic coefficient

In order to be able to interpret the concentration range for which the PS-NaPAA system behave like a suspension, the water activity as a function of water content is converted to osmotic coefficient and fitted by the model by Filho and Maurer [2008].

The osmotic coefficient is calculated for all samples of PS-NaPAA and NaPAA by using equation 4.7. To model the osmotic coefficient the fraction of free counterions must be estimated. According to [Filho and Maurer, 2008] this fraction can be obtained as the osmotic coefficient at infinite dilution. The osmotic coefficients determined from the measurement by membrane osmometry are depicted as a function of x_w in figure 7.12. The samples measured is denoted PS-NaPAA-30-M1 etc. All three samples are neutralised to a degree of more than 0.99.

As it is observed for the more concentrated solutions in figure 7.4 it is not possible to distinguish between the 30 and 40 °C. Additionally the progress for φ with x_w is different for all three samples hence all three samples is fitted with a straight line due to the lack of evidence for something more appropriate.

The fitted lines in figure 7.12 is used to calculate φ at $x_w = 1$. The values is listed in table 7.8. According to the limiting osmotic coefficient only a fraction of 0.073 of the sodium ions are free.

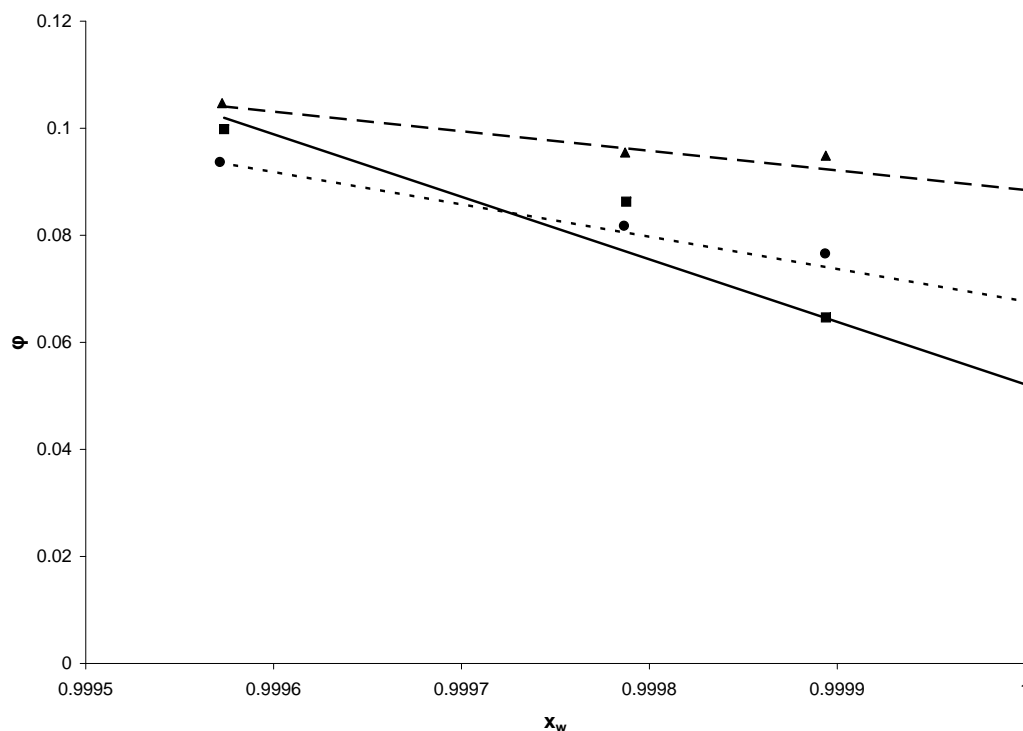


Figure 7.12: The osmotic coefficient for PS-NaPAA-30-M1 (■), PS-NaPAA-30-M2 (▲), and PS-NaPAA-40-M1 (●) along with a linear fit to PS-NaPAA-30-M1 (—), PS-NaPAA-30-M2 (---) and PS-NaPAA-40-M1 (···).

The number of monomers per polyion (r_p) corresponds to the number of charges on a completely deprotonated particles i.e. z_p , which is calculated as given in appendix A.1. The amount of particles in each sample (n_p) is calculated as described in appendix A.3. For

Table 7.8: The limiting osmotic coefficient for PS-NaPAA.

Sample	φ^{lim}
PS-NaPAA-30-M1	0.058 ± 0.008
PS-NaPAA-30-M2	0.090 ± 0.002
PS-NaPAA-40-M1	0.0707 ± 0.0004
Average	0.073

the samples of NaPAA the fraction of free counterions is obtain as the limiting osmotic coefficient as well. As NaPAA is not investigated by membrane osmometry the values from figure 7.7 is used. A straight line is fitted to the points for the osmotic coefficient below one. From the straight line the limiting osmotic coefficient is found to be 0.065 for NaPAA-30-1 and 0.012 for NaPAA-30-2 hence and average of 0.039 is used. In table 7.9 the values for the constants used in the model is depicted. It must be noted that the values for the constants A_φ , b and α is valid at 25 °C, but since no values for b and α are available at the temperature of interest, it is chosen to use the constants for 25 °C. The

Table 7.9: The constants used in the model.

	A_φ	b	α	r_p	σ
PS-NaPAA	0.3914	1.2	2	10064816	734783
NaPAA	0.3914	1.2	2	27.8	1.08

value for n_p depends on the sample and hence it is not included in table 7.9. The model is fitted to the measurements for which $\varphi < 1$ as it corresponds approximately to the range for which the model is used by Filho and Maurer [2008]. Equation 4.8 is fitted to the measurements by use of Origin (Origin 7 SR2, OriginLab Corporation). The measured osmotic coefficient along with the fitted model is given for NaPAA-30-1 and NaPAA-30-2 in figure 7.13 and 7.14 respectively. The corresponding plots for PS-NaPAA is given in figure 7.15 to 7.18.

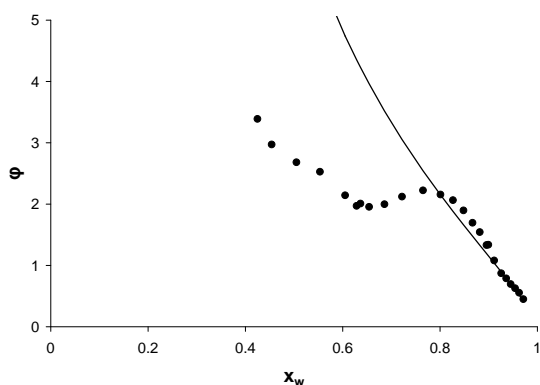


Figure 7.13: The measured osmotic coefficient for NaPAA-30-1 (●) along with the model fitted to $\varphi < 1$ (—) as a function of x_w .

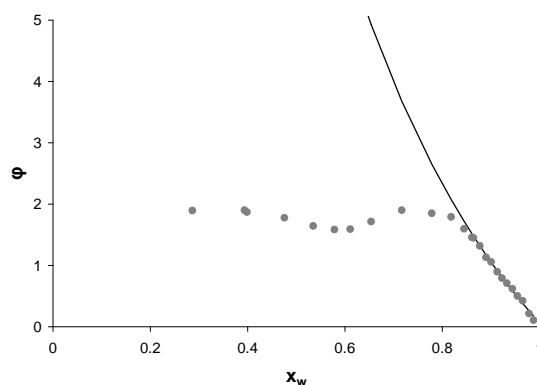


Figure 7.14: The measured osmotic coefficient for NaPAA-30-2 (●) along with the model fitted to $\varphi < 1$ (—) as a function of x_w .

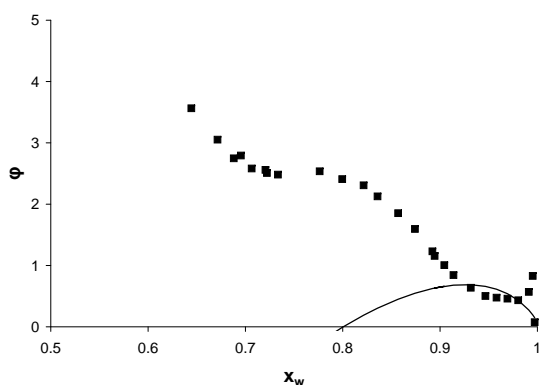


Figure 7.15: The measured osmotic coefficient for PS-NaPAA-30-1 (■) along with the model fitted to $\varphi < 1$ (—) as a function of x_w .

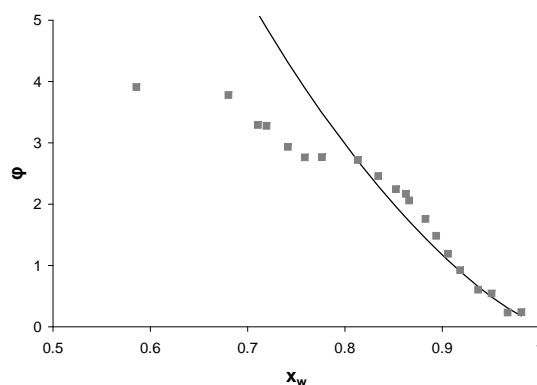


Figure 7.16: The measured osmotic coefficient for PS-NaPAA-30-2 (■) along with the model fitted to $\varphi < 1$ (—) as a function of x_w .

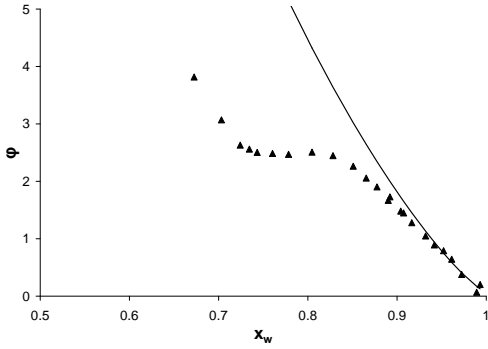


Figure 7.17: The measured osmotic coefficient for PS-NaPAA-40-1 (\blacktriangle) along with the model fitted to $\varphi < 1$ ($—$) as a function of x_w .

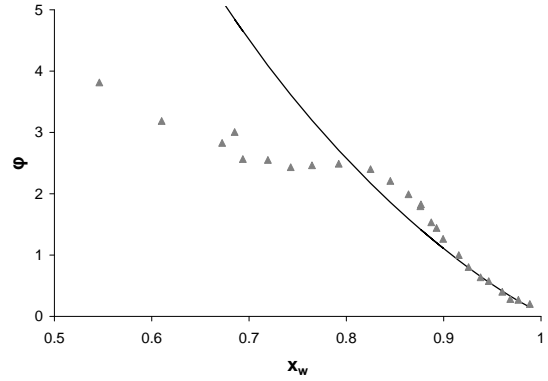


Figure 7.18: The measured osmotic coefficient for PS-NaPAA-40-2 (\blacktriangle) along with the model fitted to $\varphi < 1$ ($—$) as a function of x_w .

Figure 7.13 to 7.18 show that the model fits the measurements quite well for $\varphi < 1$ except for PS-NaPAA-30-1. The poor fit of PS-NaPAA-30-1 is due to the observed increase in φ close to one, which can not be described by the model hence PS-NaPAA-30-1 is disregarded in the following.

A quantitative measure of the quality of the fits are given by the coefficient of determination (R^2) in table 7.10. According to table 7.10 the model describe more than 95 % of the variation in the osmotic coefficient below one except for PS-NaPAA-30-1. From figure 7.13 to 7.18 it is observed that even though the model is only fitted for $\varphi < 1$ the model progress similar to the measured osmotic coefficient until a value of x_w just above the values for the bend listed in table 7.6.

Besides the values for R^2 , table 7.10 shows the fitting parameters. The fitting parameters are given as $\bar{\lambda}_{c,p}^{(k)}$ which is $\bar{\lambda}_{c,p}^{(k)} = \lambda_{c,p}^{(k)} r_p$. Hence it is possible to compare the fitting parameters for PS-NaPAA with the values for NaPAA. By comparing the values for $\bar{\lambda}_{c,p}^{(0)}$ and $\bar{\lambda}_{c,p}^{(1)}$

Table 7.10: R^2 , $\bar{\lambda}_{c,p}^{(0)}$ and $\bar{\lambda}_{c,p}^{(1)}$ along with the standard deviation of these values.

	R^2	$\bar{\lambda}_{c,p}^{(0)}$	St.dev. [%]	$\bar{\lambda}_{c,p}^{(1)}$	St.dev. [%]
NaPAA-30-1	0.9681	1.30	42	1.96	60
NaPAA-30-2	0.9806	1.94	20	-0.213	415
PS-NaPAA-30-1	-0.3538	-0.798	-166	5.55	66
PS-NaPAA-30-2	0.9535	1.62	24	-1.55	71
PS-NaPAA-40-1	0.9553	2.04	29	-1.56	98
PS-NaPAA-40-2	0.9799	1.26	15	-0.593	84
PS-NaPAA	0.8752	1.38	23	-0.598	145

for each of the fits it is observed that $\bar{\lambda}_{c,p}^{(0)}$ is in the range 1.26 to 1.94 whereas $\bar{\lambda}_{c,p}^{(1)}$ has a broader distribution. The values for NaPAA-30-1 and NaPAA-30-2 are not similar and

can not be distinguished from the parameters for PS-NaPAA. The large variation in the fitting parameters for the different samples is most likely a result of the variations between the measured water activities for the samples. This variation is enlarged by the conversion of a_w to φ as described in section 4.2.2. Hence the fitting parameters are sensitive to the experimental error observed for the determination of a_w which is confirmed by the large standard deviations for the fitting parameters. The last row in table 7.10 gives the values for a fit of the model to all φ below one for PS-NaPAA-30-2, PS-NaPAA-40-1 and PS-NaPAA-30-2. the lower value for R^2 confirms the variation in φ between the samples. Even though 18 points have been used in this fitting the standard deviation on the fitting parameters is very large.

An attempt has been made to use the model to determine the fraction of free counterions. By letting σ be a variable in the fitting of PS-NaPAA-30-2 $\sigma = 5361040 \pm 20589025$ is found. This is a standard deviation on 384 %, hence it is not possible to determine the exact value of σ from the model.

By use of equation 4.10 to 4.13 it should be possible to calculate the activity coefficients for the polyions and the counterions, but this calculation gives a very large value for $\ln\gamma$ which can not be converted to γ . Hence it is not possible to describe the activity coefficients for the sodium ions or the polyions in a quantitative manner. Thus it is only possible to note that the activity coefficients for the polyion and the sodium ions are gigantic according to the model. If the values for $\ln\gamma$ from the model are inserted into the Gibbs-Duhem equation (equation 4.4) it is observed that the activity coefficients for the sodium ions and the polyions are overestimated.

7.2.10 Fitting the BET isotherm

The measurements of water activity as a function of water content may be partly described by the theory of adsorption given in section 4.3 on page 18.

The measured values for a_w as a function of water content given in e.g. figure 7.4 resembles type II or III adsorption. This kind of adsorption can be described by the BET isotherm as described in section 4.3.2. Hence a_w as a function of Y is fitted with the inverted BET isotherm by use of Origin (Origin 7 SR2, OriginLab Corporation). The initial guesses for c and Y_{mono} were 10 and 0.01 respectively. An example for a fit is seen in 7.19, where the measurements for PS-NaPAA-30-2 is used.

In figure 7.19 it is seen that the inverted BET isotherm fits the measured a_w the best in the range $0 < Y < 0.3$. Above this range the inverted BET isotherm underestimates the value for a_w . Figure 7.19 is representative for all sample of PS-NaPAA, NaPAA and PS-PAA. If the water content as a function of the measured a_w is fitted with the ordinary BET isotherm instead, the values for a_w at high water content have a larger impact on

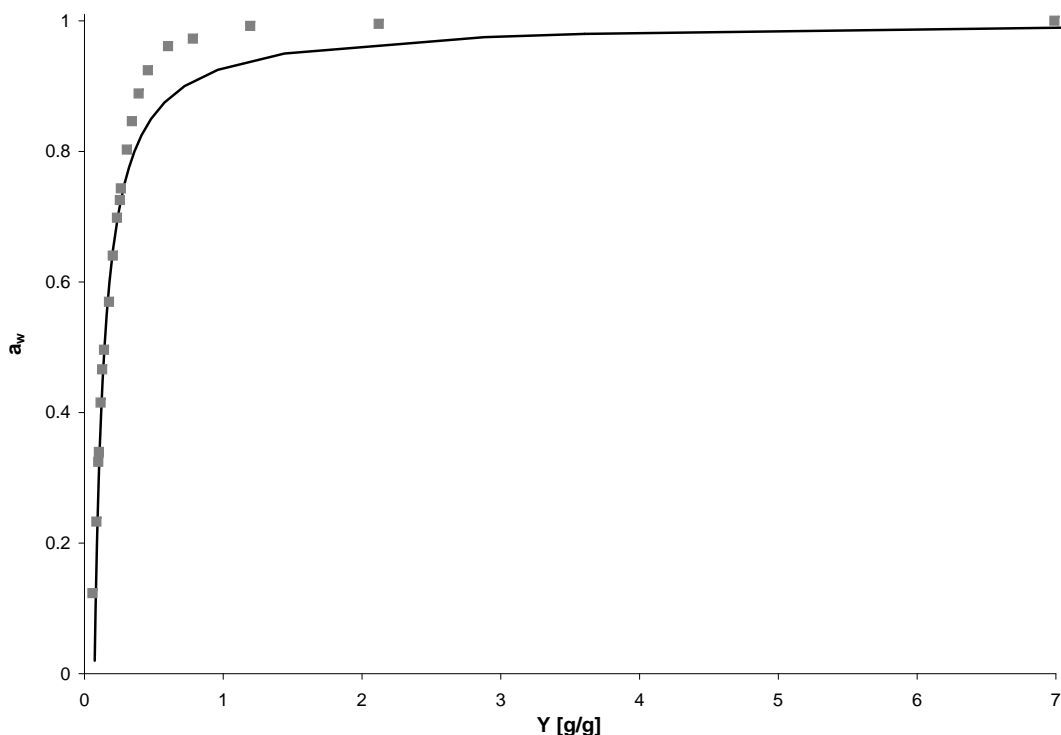


Figure 7.19: The water activity as a function of water content for PA-NaPAA-30-2 (■) fitted with the inverse BET isotherm (—).

the BET fit and hence a_w at low water content is overestimated.

The parameters obtain by fitting the inverted BET isotherm to the measured values for a_w as a function of Y , is given in table 7.11.

Table 7.11: The obtain fitting parameters for the BET isotherm.

Sample	c	St.dev [%]	Y_{mono}	St.dev [%]	R^2	$x_{w,mono}^*$
PS-NaPAA-30-1	$5.25 \cdot 10^{13}$	$3.2 \cdot 10^{13}$	0.061	2.0	0.9820	0.60
PS-NaPAA-30-2	34.5	72	0.070	4.1	0.9788	0.63
PS-NaPAA-40-1	621.5	283	0.065	2.0	0.9893	0.61
PS-NaPAA-40-2	20.7	45	0.061	3.9	0.9827	0.61
NaPAA-30-1	8.2	26	0.224	4.8	0.9873	0.58
NaPAA-30-2	3.1	19	0.219	6.0	0.9890	0.57
PS-PAA-30-1	$1.07 \cdot 10^{45}$	104	0.021	13.1	0.7282	
PS-PAA-30-2	$2.86 \cdot 10^{44}$	665	0.020	13.5	0.8091	

For all samples of PS-NaPAA and NaPAA $R^2 > 0.97$ as seen in table 7.11. For PS-PAA R^2 is lower. As seen in table 7.11 Y_{mono} is approximately 0.06 for the PS-NaPAA particles where as Y_{mono} is only 0.02 for PS-PAA. For NaPAA Y_{mono} is larger than both PS-PAA and PS-NaPAA. By converting the values for Y_{mono} for PS-NaPAA and NaPAA into x_w^* which is given in the last coloumn in table 7.11 it is seen that Y_{mono} for PS-NaPAA and NaPAA corresponds to the same amount of water per charge. As shown in table 7.11 the

standard deviation for Y_{mono} is relatively small, whereas the standard deviation for c is rather large. The values for c are found to vary with several orders of magnitude, but if the values for c which have a standard deviation above 100 % is disregarded c is larger for PS-NaPAA than for NaPAA.

As mentioned in section 4.3.2 on page 19 c can be used to calculate a value for $\Delta H_{des} - \Delta H_{vap}$. These values are listed in table 7.12. Disregarding PS-NaPAA-30-1

Table 7.12: $\Delta H_{des} - \Delta H_{vap}$ obtained from the values for c .

Sample	$\Delta H_{des} - \Delta H_{vap}$ [J/mol]	St.dev [%]
PS-NaPAA-30-1	79625	$1.03 \cdot 10^{12}$
PS-NaPAA-30-2	8925	20
PS-NaPAA-40-1	16746	44
PS-NaPAA-40-2	7889	15
NaPAA-30-1	5304	12
NaPAA-30-2	2872	17
PS-PAA-30-1	261335	1
PS-PAA-30-2	257998	7

$\Delta H_{des} - \Delta H_{vap}$ obtained from the BET fittings is in the order of 10000 J/mol for PS-NaPAA whereas it is slightly smaller for NaPAA. For PS-PAA $\Delta H_{des} - \Delta H_{vap}$ is approximately 20 times larger than for PS-NaPAA.

7.3 Water activity as a function of temperature

The water activity was measured as a function of temperature according to the method described in section 6.3.3 on page 29 to obtain values for ΔH_{excess} as described in section 4.3.3 on page 21. Four different samples of PS-NaPAA was investigated as a function of temperature. The degree of neutralisation is given in table 7.13.

Table 7.13: The degree of neutralisation for the samples of PS-NaPAA measured at different temperatures.

Sample	Degree of neutralisation
PS-NaPAA-T-1	0.982
PS-NaPAA-T-2	0.963
PS-NaPAA-T-3	1.02
PS-NaPAA-T-4	0.994

To verify the method described in section 6.3.3 on page 29 a_w measured at 35 °C is plotted as a function of the average water content for each measurement series in figure 7.20 together with a_w for PS-NaPAA-30-2.

According to figure 7.20 a_w measured for the four samples at $T = 35$ °C resemble the

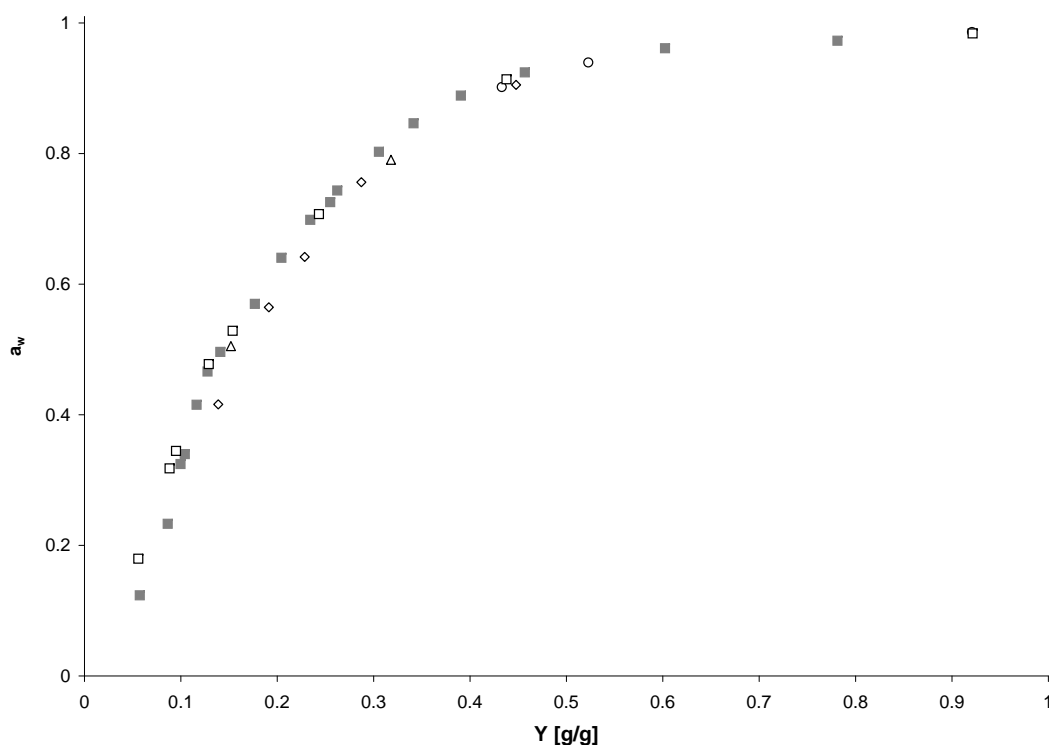


Figure 7.20: Water activity as a function of water content for PS-NaPAA-T-1 (Δ), PS-NaPAA-T-2 (\diamond), PS-NaPAA-T-3 (\circ) and PS-NaPAA-T-4 (\square) along with the water activity for PS-NaPAA-30-2 (\blacksquare).

corresponding a_w for PS-NaPAA-30-2. The deviation between the samples is in the same range as the deviation observed in figure 7.4 on page 37. Hence the method for measuring a_w as a function of temperature gives values similar to the values obtained by the method for varying water content.

The excess enthalpy is calculated according to equation 4.21 on page 22. The values obtained are listed in table 7.14 along with the standard deviation in percentage obtained from the fitting. The weighing before and after each measurement series indicate a change in x_w during each measurement series. The change in x_w is generally below 5 % as it is seen in table 7.14. Even though the change in x_w is small it still affects the value of ΔH_{excess} , hence a corrected value for ΔH_{excess} is calculated by subtracting the contribution from the change in x_w . The x_w given in table 7.14 is an average of the x_w before and after each measurement series.

A negative value for ΔH_{excess} means that the water has a favourable interaction with PS-NaPAA i.e. more energy is required to remove the water from the PS-NaPAA. Table 7.14 shows that a higher x_w results in a less negative ΔH_{excess} . The standard deviation in percentage for ΔH_{excess} is generally increases as ΔH_{excess} becomes less negative. $\Delta H_{excess}^{corrected}$ is generally more negative than ΔH_{excess} at the same x_w . The only exception is for PS-NaPAA-T-4 at $x_w=0.58$ at which $\Delta H_{excess}^{corrected}$ is more negative than ΔH_{excess}

Table 7.14: The ΔH_{excess} obtained at the given x_w for four different samples. The change in x_w is given along with a value for ΔH_{excess} which is corrected for the contribution from the change in x_w .

Sample	x_w	ΔH_{excess} [J/mol]	%SD	Change in x_w [%]	$\Delta H_{excess}^{corrected}$ [J/mol]
PS-NaPAA-T-1	0.79	-2836	1.4	3.4	-3746
PS-NaPAA-T-1	0.89	-442	5.7	1.9	-951
PS-NaPAA-T-2	0.78	-5053	4.6	4.4	-6241
PS-NaPAA-T-2	0.83	-1739	2.5	2.8	-2475
PS-NaPAA-T-2	0.86	-1142	1.8	2.5	-1796
PS-NaPAA-T-2	0.88	-541	5.4	1.7	-985
PS-NaPAA-T-2	0.92	-519	11.4	1.2	-963
PS-NaPAA-T-3	0.91	-475	14.2	1.4	-848
PS-NaPAA-T-3	0.93	-327	8.3	0.8	-550
PS-NaPAA-T-3	0.96	-277	21.1	0.4	-394
PS-NaPAA-T-3	0.99	-88	55.1	0.0	-98
PS-NaPAA-T-4	0.58	-10999	6.7	-14.1	-7548
PS-NaPAA-T-4	0.70	-5815	3.5	4.3	-6958
PS-NaPAA-T-4	0.69	-4123	1.8	3.3	-4998
PS-NaPAA-T-4	0.76	-3286	2.6	4.0	-4346
PS-NaPAA-T-4	0.79	-2408	1.5	3.5	-3342
PS-NaPAA-T-4	0.86	-883	6.2	1.9	-1395
PS-NaPAA-T-4	0.92	-322	11.3	0.9	-548
PS-NaPAA-T-4	0.96	-316	18.3	0.3	-389

due to water condensation on the sample during the measurement series. Both ΔH_{excess} and $\Delta H_{excess}^{corrected}$ at this x_w should not be emphasised too much as the change in x_w during this measurement series is 14.1 % and hence the assumption of constant x_w is rather questionable.

In general the correction of ΔH_{excess} is less precise than ΔH_{excess} itself as the correction is calculated based on the weighing before and after each measurement series i.e. only two points whereas ΔH_{excess} is based on seven measurements. Figure 7.21 on the next page shows ΔH_{excess} as a function of x_w .

According to figure 7.21 ΔH_{excess} measured for the four samples of PS-NaPAA is of comparable magnitude. The only value for ΔH_{excess} which deviates considerably between two sample is ΔH_{excess} for $x_w = 0.78$ for PS-NaPAA-T-2 which is significantly more negative than the corresponding measurements for PS-NaPAA-T-4 at $x_w = 0.79$. Within the values for ΔH_{excess} for PS-NaPAA-T-4 the values at $x_w = 0.69$ and $x_w = 0.70$ differ significantly as ΔH_{excess} at $x_w = 0.69$ is almost 30 % less negative than ΔH_{excess} at $x_w = 0.70$ even though a more negative value at $x_w = 0.69$ is expected due to the measurement at $x_w = 0.58$ and the general behaviour of ΔH_{excess} as a function of x_w . The measurement series at $x_w = 0.69$ is made after the sample had been stored for a night and no addi-

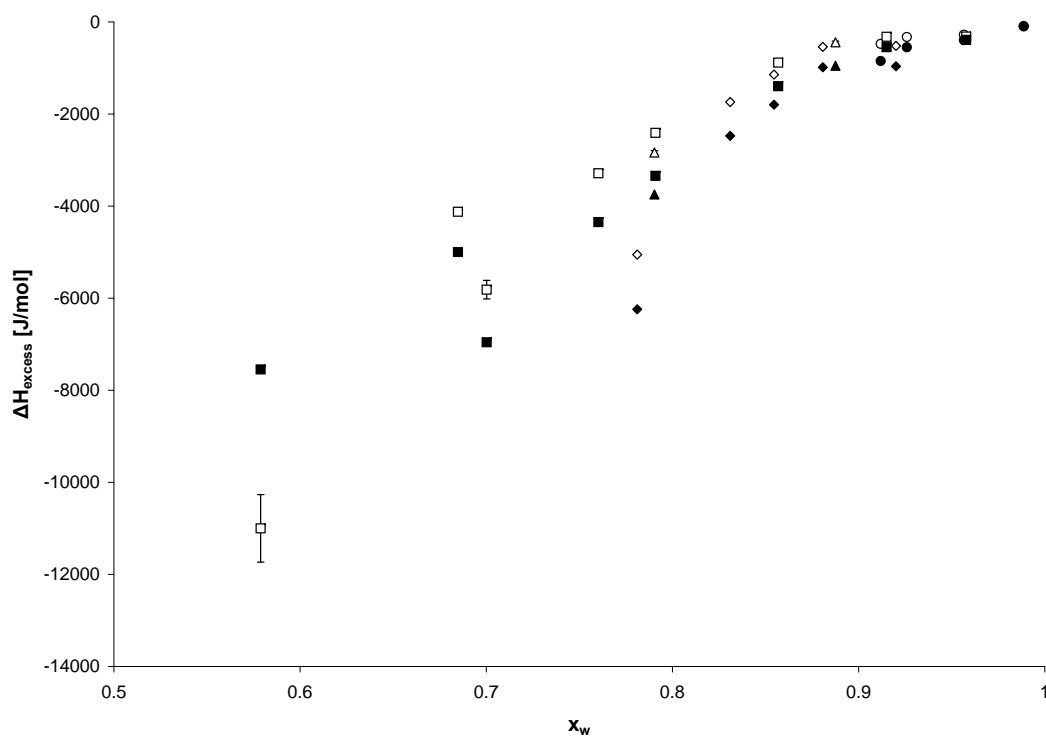


Figure 7.21: ΔH_{excess} as a function of x_w for PS-NaPAA-T-1 (\triangle), PS-NaPAA-T-2 (\diamond), PS-NaPAA-T-3 (\circ) and PS-NaPAA-T-4 (\square) along with $\Delta H_{excess}^{corrected}$ for PS-NaPAA-T-1 (\blacktriangle), PS-NaPAA-T-2 (\blacklozenge), PS-NaPAA-T-3 (\bullet) and PS-NaPAA-T-4 (\blacksquare)

tionally water has been added before the measurement series. The measurement series at $x_w=0.69$ are the only measurement series at which no additional water is added after storage. According to figure 7.20 a_w at $x_w=0.69$ do not deviate considerably from the other measurements for a_w .

7.4 Drying of poly(styrene-*co*-sodium acrylate)

Two samples of PS-NaPAA was dried at 40 °C using simultaneous thermal analysis.

The PS-NaPAA investigated has a degree of neutralisation of 0.994.

Figure 7.22 shows the calculated flux for the two measurements as a function of the water content. The flux is proportional to the water activity. According to figure 7.22 the flux increases with increasing water content. The flux has a rather large fluctuation, which is partly a result of the numeric differentiation. The flux is reproduced for the two measurements. As seen in figure 7.22 no distinct bends or changes in the flux as a function of water content is observed.

Figure 7.23 shows the energy per mass loss as a function of water content. The energy

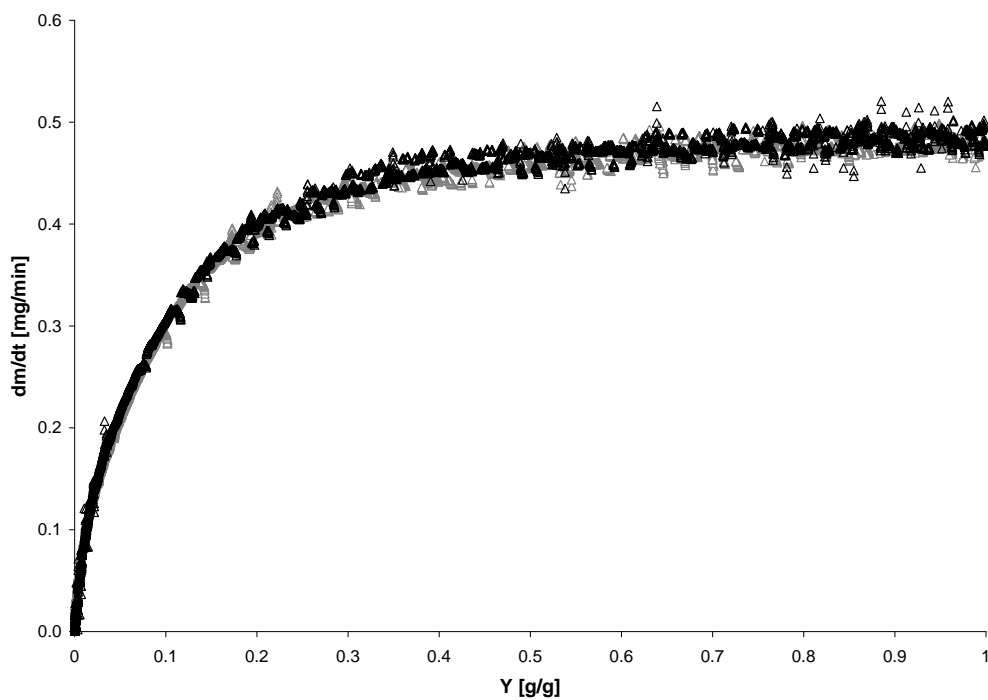


Figure 7.22: The flux in mass loss as a function of water content for two measurement series for PS-NaPAA (\triangle and \triangle).

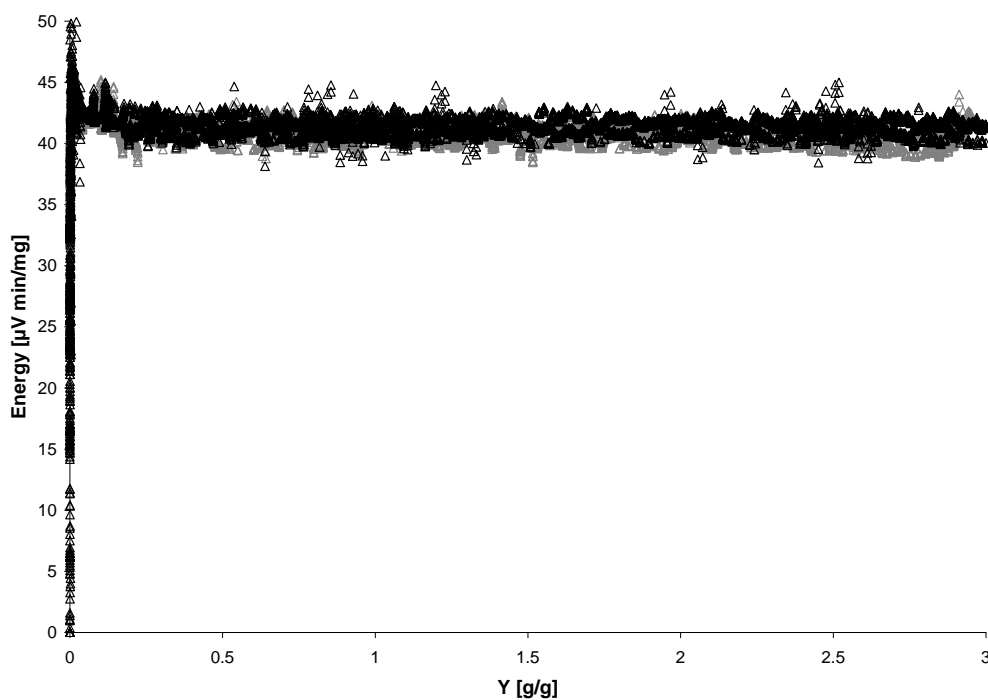


Figure 7.23: The energy input per mass loss as a function of water content for two measurement series for PS-NaPAA (\triangle and \triangle).

input per mass loss is observed to increase slightly when Y approaches zero. For $Y < 0.02$ the energy input per mass loss shows both very high and very low values. These values is assumed to be a result of the computation process and not a result of the reality.

8. Discussion

8.1 Validation of methods

As described in section 7.2.1 the measurements of a_w may not be accurate since a sample of PS-NaPAA with longer time to equilibrate is measured to have a slightly lower a_w than the PS-NaPAA samples measured using the ordinary method. Hence a stable value for a_w in a measurement only indicate that equilibrium between the sample and the air is established whereas the internal equilibrium between e.g. PS-NaPAA and water is not necessarily established. Though the measured a_w is assumed to reflect the reality since it is possible to reproduce the tendencies for a_w as a function of water content for all samples within a certain error margin. Additionally the sample measured over a period of 19 days seems to follow the same tendency as the measurements of the remaining samples. The fact that less than 25 % of the water evaporated from the samples during a measurement series can be described by the evaporation of water to reach the measured a_w , is a proof of evaporation of water somewhere else in the process. The water can evaporate either after addition of water and before the measurement, during the measurement, after the measurement before weighing or after weighing and before addition of more water. Since the samples are measured at temperatures above room temperature the warm sample is believed to evaporate more water than is expected for a sample at room temperature. Thus the evaporation of water is most pronounced after measurement before weighing as this is the period where the temperature difference between the sample and the surroundings is largest. If this is the case all the measured values for Y are lower than the actual water content in the sample at the time of the a_w measurement. The fact that the evaporation of water from the samples at 40 °C is similar to the samples at 30 °C according to table 7.3 counteract this explanation since more water should be evaporated from a sample at 40 °C due to the above explanation. It is only if water evaporates after measurements before weighing that the value for Y do not correspond to the measured a_w . It is not possible to determine in which part of the process the evaporation of water is most pronounced.

The small deviations between samples measured at the same temperature and water content may be a result of the evaporation of water.

As the measurements for PS-NaPAA at different temperatures show a change in x_w during each measurement series the values for ΔH_{excess} are not accurate as the theoretical assumption of constant x_w is not fulfilled. The correction of ΔH_{excess} is unlike to give the exact values for ΔH_{excess} since the correction assumes ideal behaviour of the evaporated

water. Though the values for ΔH_{excess} can still provide an approximate value for the extra energy needed to evaporate the water and the tendency in ΔH_{excess} as a function of x_w can still be used.

The STA method is very sensitive to the small deviations as both the flux and the energy calculated from these measurement are based on numeric differentiation of the sample loss. Neither the flux nor the energy are calibrated thus all values obtained from the STA measurements can only give an indication of whether the same trends observed for the a_w measurements is observed during the drying. Though some distinct features might be lost in the numeric differentiation since the differentiation is made over a large number of measurement points, but if the differentiation is made over fewer points the distinct features may be lost in the enlargement of the experimental uncertainty due to the numeric differentiation.

In general the used methods may not be accurate but they are able to describe the tendencies for the water activity as a function of water content and temperature.

8.2 Deviations in water activity between like samples

For the samples of PS-NaPAA, PS-NaPAA-40-1 is the only sample for which a_w deviates from the remaining samples as noted in figure 7.4. Since this tendency is not reproduced for PS-NaPAA-40-2 the deviation can not be a result of the increased temperature. The fact that a_w is slightly lower in the region $0.3 < Y < 0.8$ for PS-NaPAA-40-1 is in contrast to the results obtained from the measurements with increasing temperature for PS-NaPAA as these measurements show an increase in a_w with increased temperature. Instead the slightly lower water activity might be due to a slightly higher sodium content (cf. table 7.4). An increase in the sodium content corresponds to a lowering of x_w and theoretically to more charged groups i.e. γ_w is expected to be lower, hence a_w must be lowered. If the differences in sodium content for the samples has an observable effect, PS-NaPAA-40-2 must have a higher a_w than the other samples of PS-NaPAA as PS-NaPAA-40-2 has a lower sodium content than the other samples. Due to the assumptions in the calculation of the degree of neutrality PS-NaPAA-40-2 is actually less than 96.3 % neutralised and hence a_w for PS-NaPAA-40-2 should be even higher. Additionally the effect of temperature must in theory increase a_w for PS-NaPAA-40-2 even more. Since PS-NaPAA-40-2 is not observed to deviates significantly from the other PS-NaPAA samples it seems unlikely that the observed difference for PS-NaPAA-40-1 is caused by the the larger amount of sodium ions. Hence the deviation is assumed to correspond to an experimental error.

The difference between a_w as a function of water content measured for the two samples of NaPAA can not be attributed to the difference in degree of neutralisation since NaPAA-

30-2 has a higher a_w than NaPAA-30-1 which is the opposite order than expected due to the degree of neutralisation. The reason for the difference between the measure a_w for the two samples is more likely caused by heterogeneous samples for NaPAA. These samples is expected to be more heterogeneous than PS-NaPAA since the dried samples is not porous like the PS-NaPAA and PS-PAA samples and thus the distribution of the added water is expected to be less homogeneous.

8.3 Interpretation of a_w as function of water content

By comparing the water activity for NaPAA-30-1 and NaPAA-30-2 with the literature values given in figure 7.7 it is observed that the literature values are generally higher at the same Y. Though the model by Filho and Maurer [2008] seems to corresponds to a_w measured for NaPAA-30-1 and NaPAA-30-2. Since the molecular weight is not the same for all samples reported in figure 7.7 the level of the different measurement series should not be emphasised. The literature values show a steeper increase for PAA than for NaPAA. Additionally the values for NaPAA from Thijs and coworkers [2007] show a step increase in a_w at low Y above which a_w increase less with increasing Y. As described in section 4.4 on page 22 Thijs and coworkers [2007] interpret this bend as being a result of a conformational change of the polyion due to completion of the first hydration shell. If the bend observed for NaPAA-30-1 and NaPAA-30-2 is caused by a similar conformational change x_w^{*bend} can be interpreted as the mole fraction of water needed to complete the first hydration shell of NaPAA. As mentioned in section 7.1 on page 31 the first hydration shell on all sodium ions is complete at $x_w^* = 0.8$. x_w^{*bend} is only approximately 0.65 for NaPAA and hence only a fraction of the sodium ions should be hydrated. Additionally some of the added water must form a hydration shell around the polyacrylate ions. It is plausible that only a fraction of the sodium ions is hydrated since the sodium ions condensed on the acrylate groups are not hydrated (cf. section 4.2) and according to the charge density parameter and the limiting osmotic coefficient a part of the sodium ions must be condensed onto the polyacrylate.

For PS-NaPAA a bend is observed similar to the bend for NaPAA and hence it is interpreted analogous. For PS-NaPAA $x_w^{*bend} \approx 0.74$ which is close to the mole fraction needed to complete the first hydration shell of all present sodium ions but as for NaPAA some of the water must be used to hydrate the charged particles. Hence only a fraction of the sodium ions must be hydrated and the remaining sodium ions must be chemically associated to the acrylate groups.

For NaAc both the sodium ions and the acrylate ions must be hydrated at $Y = 1.4$ since all NaAc is observed to be dissolved at this point. If it is assumed that both the sodium

ions and the acrylate ions have one hydration shell at this point, it can be calculated that the acrylate ion must have approximately 4 water molecules in the first hydration shell. If it is further assumed that each acrylate group in the shell is similarly hydrated by four water molecules in the first hydration shell the fraction of free sodium ions can be calculated from the value of x_w^{*bend} . For PS-NaPAA the fraction is found to be in the range 0.31 to 0.39. For NaPAA the fraction of free counterions is calculated to be in the range 0.21 to 0.25. These values should be use with caution since they are based on the mentioned assumptions. Additionally it should be noted that even though the interpretation of the bend is given by Thijs and coworkers [2007], they present no evidence for this interpretation.

The interpretation of the bend as corresponding to formation of the first hydration shell is partially supported by the fitting of the Filho and Maurer model to the measurements. Even though the model is only fitted in the range where $\varphi < 1$ the models is observed to progress similar to the measurements for $x_w > x_w^{*bend}$ (approximately). The model is based on solution theory but the model have limited physical interpretation due to the large variation in the fitting parameters. However it still describe the behaviour of φ for suspensions of PS-NaPAA and solutions of NaPAA since the model is fitted in a concentration range for which PS-NaPAA is in suspension and NaPAA in solution. Hence the part of the measurements which do not progress similar to the model may be the region in which PS-NaPAA and NaPAA is not hydrated and hence can not be described as a suspension/solution.

On the contrary the interpretation of the observed bends as the point, where the first hydration layer is formed, is in contradiction to the values for Y_{mono} obtained from fitting the BET isotherm to the measured a_w . According to the values for Y_{mono} the first hydration shell is formed at lower x_w^* than the observed bend.

By comparing Y_{mono} for PS-PAA and for PS-NaPAA it is observed that more water is needed to complete the first hydration shell for PS-NaPAA than for PS-PAA. This difference is caused by the hydration of the sodiums ions which are not present in PS-PAA. Additionally the charged acrylate groups may have more water in the first hydration shell than an uncharged acrylic acid group.

The values for $x_{w,mono}^*$ for PS-NaPAA and NaPAA is approximately the same. Hence the same amount of water is needed to hydrate the same amount of charges and corresponding sodium ions. This seems plausible since the PS core is found to have no impact on the water activity. Though the uncharged acrylic acid groups on NaPAA should increase the amount of water needed for the first hydration shell since PS-PAA is observed to have $Y_{mono} \neq 0$.

No bend similar to the bend observed for a_w vs. Y for NaPAA and PS-NaPAA is observed for the flux in the STA measurements. Since the bend is observed to be independent of

the relative humidity of the surrounding and the day to day storage (cf. appendix D), the lack of bend in the drying measurements can be due to differences in the behaviour of the desorption and the adsorption. Alternatively the drying curve may actually contain a bend but the bend is diminished due to the numeric differentiation.

8.4 The different parts contribution to a_w

As mentioned earlier bare polystyrene particles do not influence the water activity at all. According to figure 7.9 the water activity is considerably lower for PS-NaPAA than for PS-PAA at the same water content. Hence the sodium ions and the charged acrylate groups contribute more to a_w than the particles as a whole. This tendency is similar to the tendency for a_w for PAA and NaPAA reported in the literature as seen from figure 7.7.

The NaPAA and the PS-NaPAA samples have approximately the same a_w at the same x_w^* above $x_w^* \approx 0.9$. The differences between the NaPAA in the shell and free NaPAA is the presence of uncharged acrylic acid groups on the free NaPAA, the lower molecular weight of the free NaPAA and the fact that NaPAA in the shell is anchored to the core. The latter implies that the local concentration of charged groups and counterions are larger in the shell than for free NaPAA, when the water content is so large that bulk water is present. According to table 7.2 bulk water is only present above $x_w \approx 0.97$ thus a difference due to differences in the local concentration of NaPAA should only be present above $x_w \approx 0.97$. No difference is observed in this range. Thus the observed difference between PS-NaPAA and NaPAA at low x_w^* is mainly attributed to the presence of uncharged acrylic acid groups which is expected to be less hydrated. This is in agreement with the fact that free NaPAA has a higher a_w at the same value for x_w^* corresponding to the higher a_w reported for PAA compared to NaPAA in the literature.

The difference in size between the free and the bound NaPAA is assumed to have a minor effect as a_w for free NaPAA is higher than for PS-NaPAA whereas the opposite effect is expected if the size has an effect. Though the PS-NaPAA might have an additional contribution to a_w since the NaPAA is unable to move freely. This additional contribution is believed to be partly entropy related and hence it may be observed if the correct position of x_w^{*bend} and the corresponding a_w is known for both free NaPAA and PS-NaPAA (both completely neutralised). These values will give an indication of both the differences in entropy, through the chemical potential calculated from a_w , and how much water is needed to complete the first hydration shell and hence it is possible to get an idea of the relative higher or lower fraction of free counterions in the PS-NaPAA compared with free NaPAA. A comparison of NaPAA and PS-NaPAA with NaAc shows that a_w is similar to both

NaPAA and PS-NaPAA above $x_w = 0.9$. This similarity is also observed for γ_w and hence the interaction between water and the sodium and acrylate ions resemble the interaction between water and the sodium and polyacrylate ions.

For all NaPAA and PS-NaPAA γ_w is above one for x_w above approximately 0.9. This range corresponds to the range for which φ is below one. According to Manning [1969] φ below one is a result of both counterion condensation and Debye-Hückel interaction between the counterions and polyelectrolytes. Additionally a_w is also known to depend on the hydration of the solutes [Vlachy, 2008]. Hence the behaviour of γ_w can be interpreted as a combination of the hydration of the sodium ions and the polyelectrolytes and the interactions between the counterions and the polyion. Since the part of the water which has strong interactions with the polyion and the sodium ions is comparable smaller at high x_w the interactions between the sodium ions and the acrylate groups are more pronounced at high x_w whereas the strong interactions between water and the sodium ions and the polyions have a larger impact on γ_w at low x_w . For all samples γ_w approach one as x_w approach one, hence ideality is approached for dilute solutions/suspensions.

From the above discussion it is reasonable to presume that the water activity of PS-NaPAA is determined mainly by the charges in the shell along with the sodium ions. At least for relative diluted samples ($x_w > 0.9$) a_w and γ_w for PS-NaPAA corresponds to a_w and γ_w for NaPAA and NaAc at the same sodium ion content. A protonated shell has an impact on the water activity whereas the PS core has no influence at all.

8.5 Interpretation of the osmotic coefficient

If the interpretation of φ given by Das and coworkers [2002] is used on the values for φ given in figure 7.12 less than 10 % of the counterions are free to move outside the shell of the particles, which is slightly higher than the fraction observed for polystyrene-poly(sodium styrenesulfonate) by Das and coworkers [2002]. The small difference may be a result of the different particles investigated along with the fact that the measurements by Das and coworkers [2002] is conducted on ten times more diluted samples. Though the interpretation of φ given by Das and coworkers [2002] is contrary to the interpretation given by Manning [1969] as described above.

As mentioned earlier the variation in the fitting parameters in the model by Filho and Maurer [2008] is a result of the experimental errors which are magnified by conversion of a_w to φ . Since the fitting parameters are very sensitive to the experimental variation, no information about NaPAA and PS-NaPAA can be interpreted from the values of the fitting parameters. Additionally it is noted that the values for $\bar{\lambda}_{c,p}^{(0)}$ is approximately 10 times larger than the value obtained by Filho and Maurer [2008] whereas $\bar{\lambda}_{c,p}^{(1)}$ is both

higher and lower than the value reported by Filho and Maurer [2008]. This confirms the fitting parameters sensitivity toward experimental variations. When a_w calculated from the fitting parameters obtained by Filho and Maurer [2008] is observed to have no noticeable difference from the measured a_w for NaPAA (cf. figure 7.7) this is a result of the magnification of differences when converting a_w to φ .

8.6 The excess enthalpy

The excess enthalpy reported in section 7.3 is the excess enthalpy released during adsorption of water vapour to PS-NaPAA i.e. the numerical value of ΔH_{excess} is the excess enthalpy needed to evaporate water from a sample of PS-NaPAA.

As described in section 7.3 ΔH_{excess} becomes more negative with decreasing x_w . This behaviour is caused by the fact that ΔH_{excess} is given per mole water and at lower x_w a larger part of the water is positioned in the first hydration shell and hence more energy is needed to remove this water from the sample.

As mentioned in section 7.3 ΔH_{excess} at $x_w = 0.69$ is less negative than expected. The only difference between this measurement and the remaining samples is that this sample has been stored for the night. During this storage period the interaction between PS-NaPAA and water in the sample should come closer to the equilibrium interaction. It is expected that the interactions between PS-NaPAA and water will be stronger as the sample approach equilibrium since the water will be more evenly distributed and a_w is observed to be lowered when approaching equilibrium (cf. section 7.2.1). Hence ΔH_{excess} is expected to decrease when equilibrium is approached. This is in contrast to the observed change in ΔH_{excess} , thus the change in ΔH_{excess} can not be explained by a difference in the degree of equilibrium.

Only three measurements are present below x_w^{*bend} and since at least two of these points are uncertain due to a not constant x_w and the above described deviation, it is not possible to determine if the progress in ΔH_{excess} as a function of x_w is different below x_w^{*bend} . $\Delta H_{des} - \Delta H_{vap}$ determined from the fitting of the BET isotherm is an average value for the excess enthalpy necessary to evaporate water from the given sample, which applies to the range at which the BET isotherm fits the measurements. Since the BET isotherm fits the measurements best at low water content it is expected that $\Delta H_{des} - \Delta H_{vap}$ is in the same range as ΔH_{excess} at low x_w which is in fact the case. In theory the values for $\Delta H_{des} - \Delta H_{vap}$ should be numerically smaller than ΔH_{excess} at the lowest x_w , but $\Delta H_{des} - \Delta H_{vap}$ is observed to be slightly higher. This difference can be ascribed to heterogeneities in the particles or any entropic contribution as described in section 4.3.2.

A comparison of the values for $\Delta H_{des} - \Delta H_{vap}$ for PS-NaPAA and NaPAA shows a slightly

lower value for NaPAA. This may be due to the presence of uncharged acid groups on NaPAA which has less interaction with water as seen in figure 7.7. Additionally the fact that the NaPAA chains in the PS-NaPAA particles are fixed to the core may contribute to a higher value for $\Delta H_{des} - \Delta H_{vap}$.

According to table 7.12 $\Delta H_{des} - \Delta H_{vap}$ for PS-PAA is approximately 20 times larger than for PS-NaPAA. It is unlikely that the uncharged PS-PAA samples demand more energy to evaporate the water than PS-NaPAA, since all other measurements show that PS-PAA has less interaction with water than PS-NaPAA. Hence the large value for $\Delta H_{des} - \Delta H_{vap}$ for PS-PAA may be a result of the relative poor fit of PS-PAA compared to PS-NaPAA and NaPAA as R^2 is larger for PS-NaPAA and NaPAA than for PS-PAA.

According to figure 7.23 for the drying experiment more energy is needed to evaporate the water from the PS-NaPAA particles as the water content is decreased. This is in agreement with the values obtained for ΔH_{excess} .

Thus the use of water activity measurements to determine the excess enthalpy necessary to evaporate water from the samples seems to be a usable method even though some refinements should be made in order to determine the accurate values for ΔH_{excess} .

9. Conclusion

For the polyelectrolyte core-shell particles of poly(styrene-*co*-sodium acrylate) measurements of water activity at various concentration show that the water activity is mainly a result of the interactions between the charges and counterions in the shell.

From the measurements of water activity as a function of water content it is possible to determine the concentration range in which the interaction between water and the polyelectrolyte core-shell particles is described by adsorption and the concentration range in which the samples of core-shell particles can be regarded as suspensions. If the point where the water activity for the samples of core-shell particles change from being described by adsorption to be described as a suspension is accurately determined it is possible to estimate the fraction of free counterions in concentrated solutions/suspensions. Though additional experiments is necessary to verify that the assumptions used to determine this point are valid.

The measurements of water activity as a function of temperature provides information of the excess enthalpy necessary to evaporate the water from samples of core-shell particles. The magnitude of these excess enthalpies is confirmed by the enthalpy derived from the fit of the BET isotherm to the measured water activity as a function of water content. The tendency in the excess enthalpies as a function of water content is partly confirmed by the energy demands for isothermal drying of a sample of core-shell particles.

Thus it is concluded that measurements of water activity for systems of polyelectrolyte core-shell particles and water can provide information of the interactions between water and polyelectrolyte core-shell particles.

Bibliography

- [Atkins and de Paula, 2002] Atkins, P. and de Paula, J. (2002). *Physical chemistry*. Oxford University Press, 7th edition.
- [Blandamer et al., 2005] Blandamer, M. J., Engberts, J. B. F. N., Gleeson, G. T., and Reis, J. C. R. (2005). Activity of water in aqueous systems; a frequently neglected property. *Chemical Society Reviews*, 34(5):440–458.
- [Blaul et al., 2000] Blaul, J., Wittemann, M., Ballauff, M., and Rehahn, M. (2000). Osmotic coefficient of a synthetic rodlike polyelectrolyte in salt-free solution as a test of the poisson-boltzmann cell model. *Journal of Physical Chemistry B*, 104(30):7077–7081.
- [Borget et al., 2005] Borget, P., Lafuma, F., and Bonnet-Connet, C. (2005). Interactions of hairy latex particles with cationic copolymers. *Journal of Colloid and Interfacial Science*, 284(2):560–570.
- [Chang, 2000] Chang, R. (2000). *Physical Chemistry for the Chemical and Biological Sciences*. University Science Books, 3rd edition.
- [Chaplin, 2008] Chaplin, M. (2008). Water activity. <http://www.lsbu.ac.uk/water/activity.html>, London South Bank University, visited 15/9-08.
- [Christensen, 2008] Christensen, P. V. (2008). *Online detection of aggregation processes using dielectric spectroscopy, paper 3*. PhD thesis, Aalborg University.
- [Cotton et al., 1995] Cotton, F. A., Wilkinson, G., and Gaus, P. L. (1995). *Basic Inorganic Chemistry*. John Wiley & Sons, Inc., 3rd edition.
- [Daoust and Hade, 1976] Daoust, H. and Hade, A. (1976). Effect of cationic size of heats of dilution of aqueous solution of alkaline poly(styrenesulfonates). *Macromolecules*, 9(4):608–611.
- [Das et al., 2002] Das, B., Guo, X., and Ballauff, M. (2002). The osmotic coefficient of spherical polyelectrolyte brushes in aqueous salt-free solution. *Progress in Colloid and Polymer Science*, 121:34–38.
- [Decagon Devices, Inc, 2008] Decagon Devices, Inc (2008). *Operator's Manual AquaLab 4 Water Activity Meter*.

- [Dingenouts et al., 2004] Dingenouts, N., Patel, M., Rosenfeldt, S., Pontoni, D., Narayanan, T., and Ballauff, M. (2004). Counterions distribution around a spherical polyelectrolyte brush probed by anomalous small-angle x-ray scattering. *Macromolecules*, 37(21):8152–8159.
- [DS 204, 1980] DS 204 (1980). *Dansk Standardiseringsråd, Vandundersøgelse: Tørstof og gløderest*, 1st edition.
- [Dubreuil and Guenoun, 2001] Dubreuil, F. and Guenoun, P. (2001). Polyelectrolyte tethered to a free surface. *European Physical Journal E*, 5(1):59–64.
- [Ellerbrock et al., 2005] Ellerbrock, R. H., Gerke, H. H., Bachmann, J., and Goebel, M. O. (2005). Composition of organic matter fraction for explaining wettability of three forest soils. *Soil Science Society of America Journal*, 69(1):57–66.
- [Fernandez et al., 1995] Fernandez, D. P., Goodwin, A. H. P., and Sengers, J. M. H. L. (1995). Measurements of the relative permittivity of liquid water at frequencies in the range of 0.1 to 10 khz and at temperature between 273.1 and 373.2 k at ambient pressure. *International Journal of Thermophysics*, 16(4):929–955.
- [Filho and Maurer, 2008] Filho, P. d. A. P. and Maurer, G. (2008). An extension of the pitzer equation for the excess gibbs energy of aqueous electrolyte systems to aqueous polyelectrolyte solutions. *Fluid Phase Equilibria*, 269(1-2):25–35.
- [Fritz et al., 2002] Fritz, G., Schädler, V., Villenbacher, N., and Wagner, N. J. (2002). Electrosteric stabilization of colloidal dispersions. *Langmuir*, 18(16):6381–6390.
- [Groenewegen et al., 2000] Groenewegen, W., Lapp, A., Egelhaff, S. U., and van der Maarel, J. R. C. (2000). Counterions distribution in the coronal layer of polyelectrolyte diblock copolymer micelles. *Macromolecules*, 33(11):4080–4086.
- [Guo and Ballauff, 2000] Guo, X. and Ballauff, M. (2000). Spatial dimensions of colloidal polyelectrolyte brushes determined as by dynamic light scattering. *Langmuir*, 16(23):8719–8726.
- [Guo and Ballauff, 2001] Guo, X. and Ballauff, M. (2001). Spherical polyelectrolyte brushes: comparison between annealed and quenched brushes. *Physical Review E*, 64(5):051406.
- [Hiemenz and Rajagopalan, 1997] Hiemenz, P. C. and Rajagopalan, R. (1997). *Principles of Colloid and Surface Chemistry*. Marcel Dekker, Inc., 3rd edition.

- [Hinge, 2006] Hinge, M. (2006). *Synthesis of soft shell poly(styrene) colloids for filtration experiments*. PhD thesis, Aalborg University.
- [Hiraoka et al., 1982] Hiraoka, K., Shin, H., and Yokoyama, T. (1982). Density measurements of poly(acrylic acid) sodium salts. *Polymer Bulletin*, 8(7-8):303–309.
- [Hwang et al., 1998] Hwang, S., Kim, J., and Yoo, K.-P. (1998). Vapor liquid equilibrium data of binary polymer solutions by vacuum electromicrobalance. *Journal of Chemical and Engineering Data*, 43(4):614–616.
- [Kan et al., 2001] Kan, C. Y., Kong, X. Z., Yuan, Q., and Liu, D. S. (2001). Morphological prediction and its application to the synthesis of polyacrylate/polysiloxane core/shell latex particles. *Journal of Applied Polymer Science*, 80(12):2251–2258.
- [Lide, 2009] Lide, D. R., editor (2009). *Physical Constants of Organic Compound*, in *CRC Handbook of Chemistry and Physics*. CRC Press/Taylor and Francis, Boca Raton, FL, 89. edition. (Internet Version 2009).
- [Lyklema, 1995] Lyklema, J. (1995). *Fundamentals of Interface and Colloid Science. Volume II: Solid-Liquid Interfaces*. Academic Press.
- [Manning, 1969] Manning, G. S. (1969). Limiting laws and counterion condensation in polyelectrolyte solutions i. colligative properties. *The Journal of Chemical Physics*, 51(3):924–933.
- [Manning, 1984] Manning, G. S. (1984). Limiting laws of counterion condensation in polyelectrolyte solutions. 8. mixtures of counterions, species selectivity and valency selectivity. *Journal of Physical Chemistry*, 88(26):6654–6661.
- [McMurry, 2003] McMurry, J. (2003). *Fundamentals of Organic Chemistry*. Thomson Brooks/Cole, 5th edition.
- [Money, 1989] Money, N. P. (1989). Osmotic pressure of aqueous polyethylen glycols: Relationship between molecular weight and vapor pressure deficit. *Plant Physiology*, 91(2):766–769.
- [Mulet et al., 1999] Mulet, A., García-Reverter, J., Sanjuán, R., and Bon, J. (1999). Sorption isosteric heat determination by thermal analysis and sorption isotherms. *Journal of Food Science*, 64(1):64–68.
- [Nielsen, 2009] Nielsen, K. F. (2009). Modelling af pK_{app} 's variation for kerneskalpartikler med en skal bestående af polyacrylsyre. Master's thesis, Aalborg University.

- [Pitzer, 1973] Pitzer, K. S. (1973). Thermodynamics of electrolytes. i. theoretical basis and general equations. *The Journal of Physical Chemistry*, 77(2):268–277.
- [Rice and Nagasawa, 1961] Rice, S. A. and Nagasawa, M. (1961). *Polyelectrolyte Solution A Theoretical Introduction*. Academic Press, London and New York, 1st edition edition.
- [Semenov et al., 1999] Semenov, A. N., Vlassopoulos, D., Fytas, G., Vlachos, G., Fleischer, G., and Roovers, J. (1999). Dynamic structure of interacting spherical polymer brushes. *Langmuir*, 15(2):358–368.
- [Small et al., 2005] Small, A., Hong, S., and Pine, D. (2005). Scattering properties of core-shell particles in plastic matrices. *Journal of Polymer Science Part B Polymer Physics*, 43(24):3534–3548.
- [Stuart, 2002] Stuart, B. (2002). *Polymer analysis*. John Wiley & Sons, Ltd.
- [Thijs et al., 2007] Thijs, H. M. L., Becer, C. R., Guerrero-Sanchez, C., Fournier, D., Hoogenboom, R., and Schubert, U. S. (2007). Water uptake of hydrophilic polymers determined by a thermal gravimetric analyzer with a controlled humidity chamber. *Journal of Materials Chemistry*, 17(46):4864–4871.
- [Vlachy, 2008] Vlachy, V. (2008). Polyelectrolyte hydration: Theory and experiment. *Pure and Applied Chemistry*, 80(6):1253–1266.
- [Wu et al., 2008] Wu, Y., Ge, C., Xu, J., Bi, J., and Chen, Q. (2008). Morphologies and applied properties of psi/pa composite particles synthesized at low temperature. *Polymer Composites*, 29(11):1193–1198.

Appendix

A. Calculation of particle characteristics

In the following sections the calculation methods for different characteristics of the particles and the particle suspensions are given.

A.1 The number of particles

The mass percentage of acrylic acid incorporated is calculated according to the added amount of acrylic acid and styrene in the synthesis by use of equation A.1

$$\%AA_{inc} = \frac{V_{AA,added} \cdot \rho_{AA}}{V_{AA,added} \cdot \rho_{AA} + m_{ST,added}} \cdot 100 \quad (\text{A.1})$$

where $\%AA_{inc}$ is the mass percentage of incorporated acrylic acid, $V_{AA,added}$ is the volume of added acrylic acid, ρ_{AA} is the density of acrylic acid and $m_{ST,added}$ is the amount of styrene added to the synthesis. The density of acrylic acid is 1.0511 g/ml [Lide, 2009].

The volume of the collapsed and the swollen particles are calculated from the measured diameter of the particles.

The total volume occupied by the particles are calculated as

$$V_{tot} = \frac{m_{dm}}{\rho_{PS} \cdot (1 - \%AA_{inc}/100) + \rho_{PAA} \cdot \%AA_{inc}/100} \quad (\text{A.2})$$

where V_{tot} is the total volume of particles in 1 L suspension, m_{dm} is the dry matter content in 1 L suspension, ρ_{PS} and ρ_{PAA} are the density of PS and PAA respectively. ρ_{PS} is assumed to be 1.04 g/ml [Stuart, 2002] and ρ_{PAA} is assumed to be 1.4 g/ml [Hiraoka et al., 1982].

The number of particles is then calculated as

$$c_p = \frac{V_{tot}}{V_{col}} \quad (\text{A.3})$$

where c_p is the number of particles in 1 L suspension and V_{col} is the volume of one collapsed particle. V_{col} is calculated from the measured radius of the collapsed particle.

A.2 The size of the poly(acrylic acid) chains

The size of the PAA chains can be calculated from the thickness of the swollen shell which can be calculated if the size of the core is known. To be able to calculate the size of the core it is necessary to calculate the amount of acrylic acid in the shell. The charge density of the particles is determined to be 2.4 ± 0.05 meq/g [Nielsen, 2009]. The charge density can be converted to the ratio of acrylic acid in the shell to the total amount as

$$\%AA_{shell} = \sigma \cdot M_{AA} \quad (\text{A.4})$$

where $\%AA_{shell}$ is the mass percentage acrylic acid in the shell, σ is the charge density and M_{AA} is the molar mass of acrylic acid. The difference between $\%AA_{shell}$ and $\%AA_{inc}$ is assumed to be incorporated in to the core [Hinge, 2006].

The radius of the core is calculated from the measured radius of the collapsed particles by use of equation A.5 [Christensen, 2008].

$$r_{core} = \sqrt[3]{\frac{V_{c/s} \cdot r_{col}^3}{1 + V_{c/s}}} \quad (\text{A.5})$$

where r_{core} is the radius of the core, $V_{c/s}$ is the volume ratio of the core to the shell and r_{col} is the radius of the collapsed particle. $V_{c/s}$ is calculated as:

$$V_{c/s} = \frac{V_{ST,added} + (\%AA_{inc} - \%AA_{shell}) \cdot V_{AA,added}}{V_{AA,added} - (\%AA_{inc} - \%AA_{shell}) \cdot V_{AA,added}} \quad (\text{A.6})$$

where $V_{ST,added}$ and $V_{AA,added}$ is the volume of styrene and acrylic acid added to the synthesis respectively. for the investigated particles $V_{ST,added} = 140.9$ ml and $V_{AA,added} = 40$ ml. In equation A.6 it is assumed that the added volumes of styrene and acrylic acid corresponds to the incorporated volumes.

The thickness of the swollen shell can be calculated as

$$L_{shell} = r_{swol} - r_{core} \quad (\text{A.7})$$

where L_{shell} is the thickness of the shell and r_{swol} is the radius of the swollen particle. The poly(acrylic acid) chains have a backbone of sp^3 -hybridised carbon atoms with bond angles of approximately 109.5° [McMurry, 2003]. The distance between to neighbour carbon atoms is 154 pm [McMurry, 2003] and since each acrylic acid monomer contains two carbon atoms the length of a monomer unit can be calculated as

$$l_{AA} = \sqrt{-(\cos(109.5) - 1) \cdot 2 \cdot 154^2} \quad (\text{A.8})$$

where l_{AA} is the length of one acrylic acid monomer. The maximum molar mass of a PAA chain is then calculated as

$$M_{PAA} = \frac{L_{shell}}{l_{AA}} \cdot M_{AA} \quad (\text{A.9})$$

where M_{PAA} is the maximum molecular weight of a PAA chain.

A.3 Charges per particle

The charges pr. particles can be calculated from the charge density and the number of particles as

$$z_p = \frac{\sigma \cdot N_A \cdot m_{dm}}{c_p} \quad (\text{A.10})$$

where z_p is the number of charges per particle, σ is the charge density, m_{dm} is the dry matter content in 1 L suspension, c_p is the number of particles in 1 L suspension and N_A is Avogadro's number.

A.4 The volume of water in the shell

The volume of water in the shell is calculated as the difference between the volume of the swollen and the collapsed particle i.e.

$$V_{shell} = V_{swol} - V_{col} \quad (\text{A.11})$$

where V_{shell} is the volume of the shell i.e. the volume occupied by water, V_{swol} and V_{col} is the volume of the water swollen and the collapsed particle respectively. V_{swol} and V_{col} is calculated from the measured radii of the particles assuming that the particles are spherical.

The volume of water in the shell can be converted to the water content needed to fill all shells with water in a given sample by use of equation A.12.

$$Y_{shell} = \frac{V_{shell} \cdot \rho_w \cdot n_p}{m_{dm,s}} \quad (\text{A.12})$$

where Y_{shell} is the water content needed to fill all shells in a given sample, V_{shell} is the volume of water in a shell, ρ_w is the density of water, n_p is the number of particles in the given sample and $m_{dm,s}$ is the dry matter content of the given sample.

Similarly the mole fraction of water necessary to fill all shells in a given sample is calculated

as

$$x_{w,shell} = \frac{\frac{V_{shell} \cdot \rho_w \cdot n_p}{M_w}}{\frac{V_{shell} \cdot \rho_w \cdot n_p}{M_w} + n_{Na^+}} \quad (\text{A.13})$$

where $x_{w,shell}$ is the mole fraction of water necessary to fill all shells, M_w is the molar mass of water and n_{Na^+} is the moles of Na^+ in the sample. In equation A.13 the moles of particles are neglected since $n_p \ll n_{Na^+}$.

B. Sample stability during freeze-drying

The suspension of PS-NaPAA needs to be concentrated in order to measure the water activity in the entire concentration range. Hence it is investigated which impact freeze-drying has on the samples. Two experiments is made: one to investigate if the particles is irreversible flocculated during freeze-drying and one to study the pH in a sample of resuspended particles.

B.1 Flocculation study

B.1.1 Method

A sample of the PS-PAA suspension is adjusted to pH 11.5 (PHM200 MeterLabTM, Radiometer, Denmark. pH electrode 11, Schott Instruments, Germany) with sodium hydroxide and freeze-dried (Christ Alpha 1-2 LDplus, Germany). A part of the freeze-dried sample is resuspended in demineralised water. A small amount of this suspension is diluted with 10 mM borate buffer (pH 9.5). This suspension is used to measure the particle size by dynamic light scattering (Zetamaster, Malvern Instruments, United Kingdom). The particle size is measured three times, where each measurement consist of three sub-measurements.

For comparison PS-PAA from the stock suspension are mixed with 10 mM borat buffer (pH 9.5) to achieve two independent samples. These samples are each measured ones where each measurement consist of three subruns.

B.1.2 Results and discussion

The size measurement for non-freeze-dried sample is shown in figure B.1. From figure B.1 the average size of the particles is found to be approximately 278 nm.

The resuspended sample of freeze-dried PS-NaPAA was observed to be homogeneous. The resulting size measurements is shown in figure B.2. According to figure B.2 five out of the 9 subruns show an average diameter of approximately 277 nm. This is the same size as the size measured for the non-freeze-dried samples. Hence the freeze-dried Ps-NaPAA can be resuspended. The fact that it is not all the sub-measurements which give the same size may be due to flocculation, but since no deviation is observed in measurement 3 the

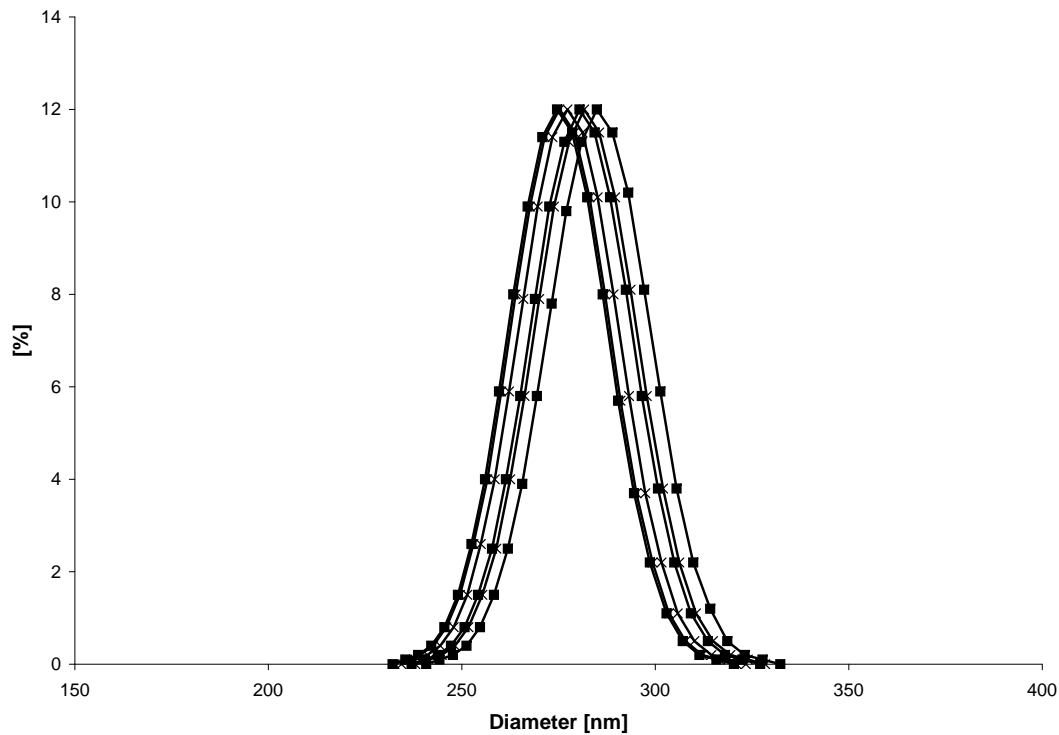


Figure B.1: The size distribution for Ps-NaPAA in 10 mM borat buffer measurement 1 (×) and 2 (■). The three peaks for each measurement correspond to the three sub-measurements.

flocculation is assumed to be reversible.

B.2 pH for resuspended poly(styrene-*co*-sodium acrylate)

B.2.1 Method

A sample of the PS-PAA suspension is adjusted to pH 9.49 (PHM200 MeterLabTM, Radiometer, Denmark. pH electrode 11, Schott Instruments, Germany) with sodium hydroxide. 4.5 ml of the sample is freeze-dried. After freeze-drying the sample is resuspended in 4.4 ml water, which corresponds to the amount of water removed during freeze-drying. The sample is stirred until the sample appears to be homogeneous and the pH is measured.

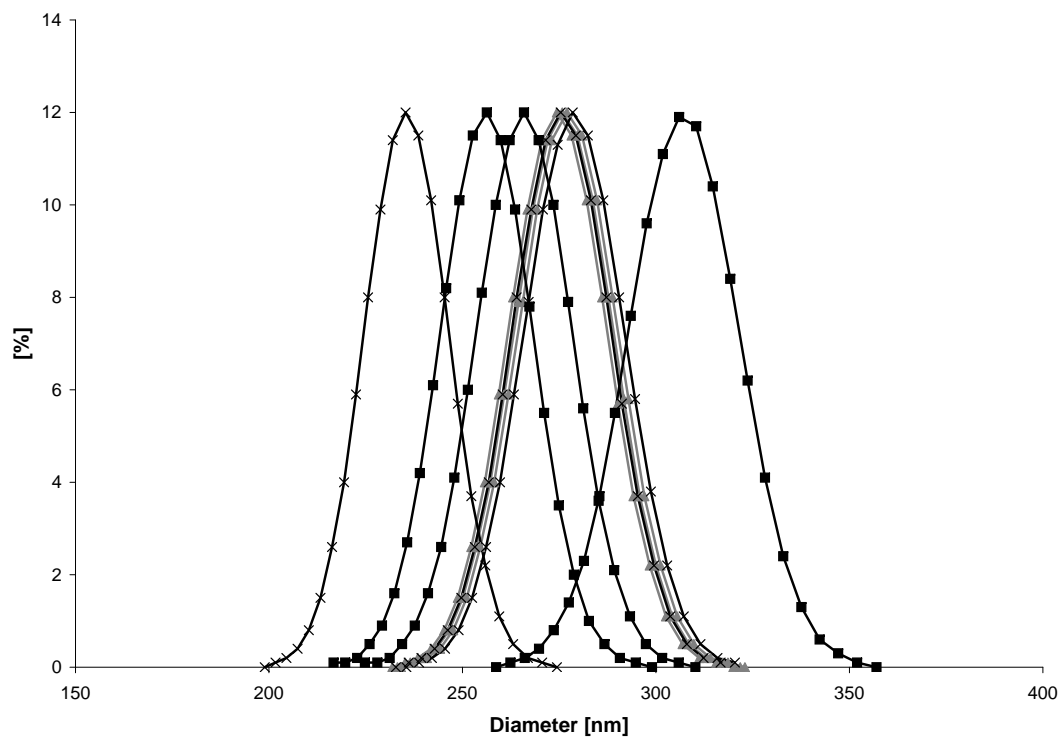


Figure B.2: The size distribution for resuspended PS-NaPAA in 10 mM borat buffer measurement 1 (×), 2 (■) and 3 (▲). The three peaks for each measurement correspond to the three sub-measurements.

B.2.2 Results and discussion

The pH of the resuspended PS-NaPAA is measured to be pH 9.43, which is approximately equal to the pH before freeze-drying.

B.3 Conclusion

Both the investigation of particle size after freeze-drying and the investigation of pH after freeze-drying show that samples of PS-NaPAA are not damaged by freeze-drying. Hence freeze-drying is a suitable method for concentrating the samples of PS-NaPAA.

C. Effect of sample storage

Since it is not possible to measure the water activity in the entire concentration range during an ordinary workday, the time dependence of the water activity was investigated. Additionally the evaporation of water during the experiment was studied.

C.1 Method

15 ml of the PS-PAA suspension was adjusted to pH 9.82 by sodium hydroxide and 10 ml of this suspension was freeze-dried in an aluminium tray. The dry sample was stored in a desiccator until it was transferred to a pre-weighed measurement cup with a pair tweezers. The sample cup is closed with a pre-weighed lid, covered with parafilm and weighed. The water activity of the sample was measured using Aqualab (Aqualab 4TE Decagon Devices, USA) and subsequently weighed. Afterwards the sample was either added a small amount (at least $2 \times 5 \mu\text{l}$) of water or the sample was stored in the closed sample cup for a given amount of time. The sample cup with sample, lid and parafilm was weighed before a new measurement.

This procedure was repeated until the water activity equals one.

The sample cup containing the sample along with the lid was dried in an oven to get an exact determination of the drymatter content.

C.2 Results

Table C.1 shows the change in the sample mass (inclusive water) during measurements and storage for a given water activity along with the corresponding storage and measurement time. According to table C.1 water is evaporating mainly during the measurement and in minor extent during storage. This is true even though the measurement time is shorter than the storage times. The amount of water evaporated during storage seems to increase with increasing storage time.

Figure C.1 shows the a_w as a function of water content for the sample of PS-NaPAA pH 9.8 $T = 30^\circ\text{C}$.

The measurements in figure C.1 is independent of the storage time since all measurements follow the same tendency.

Table C.1: The change in mass during measurement and storage for the given water activity. When no storage time is given the sample is added water and measured immediately after weighing, hence a positive $\Delta m_{storage}$ corresponds to addition of water.

storage time [hr]	$\Delta m_{measurement}$	$\Delta m_{storage}$	a_w	measurement time [min]
2	-0.0036	0.0003	0.510	37.5
	-0.0034	0.0092	0.568	29.4
7	-0.0034	-0.0008	0.517	21.1
	-0.0037	0.0096	0.596	35.7
	-0.0029	0.0079	0.647	49
2	-0.0041	-0.0002	0.609	19.7
	-0.0037	0.0077	0.653	40.3
	-0.0039	0.0081	0.701	39.2
1	-0.0037	-0.0002	0.654	19
	-0.0039	0.0087	0.707	41.7
	-0.0045	0.0091	0.753	51.2
27	-0.0034	-0.0028	0.694	17.6

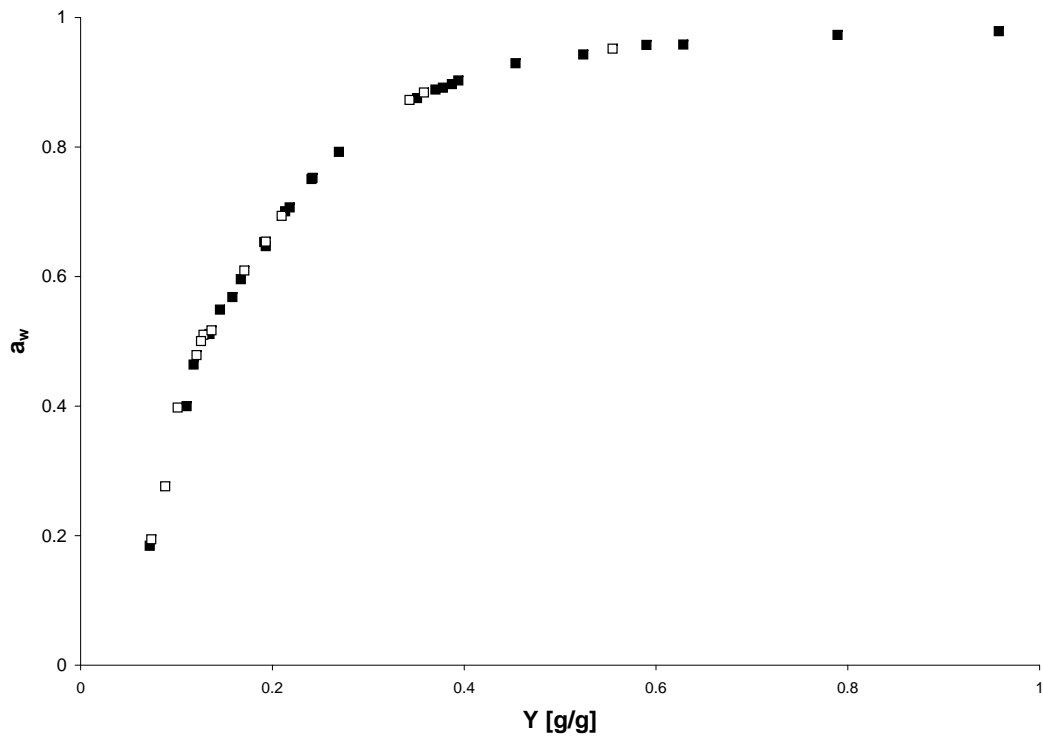


Figure C.1: The water activity (■) measured directly after water addition as a function of water content and the water activity (□) measured after 1 to 29 hours after storage as a function of water content.

C.3 Conclusion

It is necessary to weigh the samples after measuring to find the corresponding water content as part of the added water evaporates during the measurement.

The water activity depends only on the water content and not on the storage time.

D. Day of measurement

Table D.1 gives the water content and the corresponding mole fraction of water for the first measurement on day 2, 3 and 4 i.e. the water content for which the measurement of a_w may be affected by the storage of the sample over night.

Table D.1: The water content and mole fraction for the first measurement on each day of the given measurement series

Sample	Day 2		Day 3		Day 4	
	Y	x_w	Y	x_w	Y	x_w
PS-NaPAA-30-1	0.099	0.707	0.366	0.899		
PS-NaPAA-30-2	0.100	0.710	0.255	0.863		
PS-NaPAA-40-1	0.115	0.734	0.337	0.890		
PS-NaPAA-40-2	0.086	0.685	0.281	0.877		
NaPAA-30-1	0.282	0.628	1.426	0.895		
NaPAA-30-2	0.113	0.398	0.269	0.611	1.058	0.861